NASA Technical Memorandum

NASA TM - 100317

CELLULAR SOLIDIFICATION IN A MONOTECTIC SYSTEM — CENTER DIRECTOR'S DISCRETIONARY FUND FINAL REPORT

By W. F. Kaukler and P. A. Curreri

Space Science Laboratory
Science and Engineering Directorate

December 1987

National Aeronautics and Space Administration

George C. Marshall Space Flight Center

TECHNICAL REPORT STANDARD TITLE PAGE

1. REPORT NO.	2. GOVERNMENT ACCESSION NO.	3. RECIPIENT'S CATALOG NO.
NASA TM-100317		

4. TITLE AND SUBTITLE	5. REPORT DATE
Cellular Solidification in a Monotectic System – Center Director's Discretionary Fund Final Report	December 1987
	6. PERFORMING ORGANIZATION CODE
7. AUTHOR(S)	8. PERFORMING ORGANIZATION REPORT #
W. F. Kaukler and P. A. Curreri	
9. PERFORMING ORGANIZATION NAME AND ADDRESS	10. WORK UNIT NO.
George C. Marshall Space Flight Center Marshall Space Flight Center, Alabama 35812	11. CONTRACT OR GRANT NO.
	13. TYPE OF REPORT & PERIOD COVERED
12. SPONSORING AGENCY NAME AND ADDRESS	Technical Memorandum
National Aeronautics and Space Administration Washington, D.C. 20546	14. SPONSORING AGENCY CODE

15. SUPPLEMENTARY NOTES

Prepared by Space Science Laboratory, Science and Engineering Directorate.

16. ABSTRACT

Succinonitrile-glycerol, SN-G, transparent organic monotectic alloy is studied with particular attention to cellular growth. The phase diagram is determined, near the monotectic composition, with greater accuracy than previous studies. A solidification interface stability diagram is determined for planar growth. The planar-to-cellular transition is compared to predictions from the Burton, Primm, Schlichter theory. A new technique for determining the solute segregation by Fourier transform infrared spectroscopy is developed. Proposed models that involve the cellular interface for alignment of monotectic second-phase spheres or rods are compared with observation.

17. KEY WORDS	18. DISTRIBUTION STATEMENT
Monotectic Alloy, Cellular Growth, Solid/Liquid Interface Stability, Metal-Model	Unclassified – Unlimited

19. SECURITY CLASSIF. (of this report)	20. SECURITY CLASSIF. (of this page)	21. NO. OF PAGES	22. PRICE
Unclassified	Unclassified	48	NTIS

MSFC - Form 3292 (May 1969)

For sale by National Technical Information Service, Springfield, Virginia 22151

TABLE OF CONTENTS

LIST OF ILLUSTRATIONS

LIST OF ILLUSTRATIONS (Concluded)

TECHNICAL MEMORANDUM

CELLULAR SOLIDIFICATION IN A MONOTECTIC SYSTEM – CENTER DIRECTOR'S DISCRETIONARY FUND FINAL REPORT

INTRODUCTION

This research is in part directed at resolving a scientific controversy regarding alignment of the second phase particles in hypermonotectic alloys. Alternate hypotheses have been published, one by Grugel and Hellawell [1,2] and another by Parr and Johnston [3] and Schaefer et al. [4]. The Grugel and Hellawell concept proposes that the particle alignment of the second-phase liquid occurs at and behind the solidification front. Interfacial energy drives the ripening of rods of second phase into particle arrays seen in the sample after the solidification front passes (Fig. 1). The alternate hypothesis [3,4] suggests that cellular breakdown of the interface causes the second-phase liquid to collect in the aligned cell boundaries (cell cusps) which form along the local growth direction (Fig. 2).

The latter of the two mechanisms can account for some microstructural effects observed in parabolic aircraft experiments [5,6] with hypermonotectic Al-18In-xSn alloys unidirectionally grown in periods of high and low gravity. Particle alignment occurred in low-gravity sections. This can be explained by the Parr and Johnston mechanism. Gravity effects on Sn segregation could develop a Sn concentration where a change in acceleration level (along the growth axis) would result in either cellular or planar growth. Particle incorporation in the cell boundaries was noted from transverse sections.

Cellular solidification of a transparent monotectic system is systematically studied. The binary system of succinonitrile and glycerol, a transparent organic model of metallic monotectic crystallization, is utilized. Growth conditions are closely controlled and direct observation is made of the freezing front at high magnification. Thin glass cells contain the organic during unidirectional growth. Photomicrographs of the transparent interfaces are taken through these cells during solidification. By controlling the temperature gradient and growth rate, while observing the interface, the cellular breakdown of the interface (from the planar type) is determined. Conditions for the "stability diagram" are developed. The phase diagram of the system is re-evaluated. The morphology of the interfaces and solute distribution in the unidirectionally grown specimens are measured. Cellular freezing conditions in the hypermonotectic compositions within 7.5 to 16 w% are studied.

EXPERIMENTAL PROCEDURE

Organic solutions were solidified using a specially designed microscope stage. The organic solution was confined between two thin pieces of glass such that the gap between the glass slides (approximately 20 × 70 mm) was between 10 and 50 μm. The edges of the cell were sealed with quick setting epoxy (Fig. 3). The cell straddles a 0.2-cm gap between two copper blocks. The cell

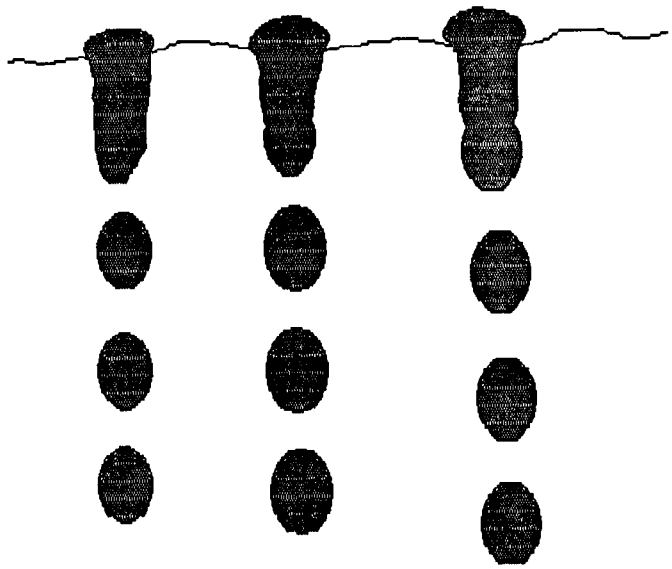

Figure 1. Schematic of the alignment monotectic mechanism proposed by Grugel and Hellawell.

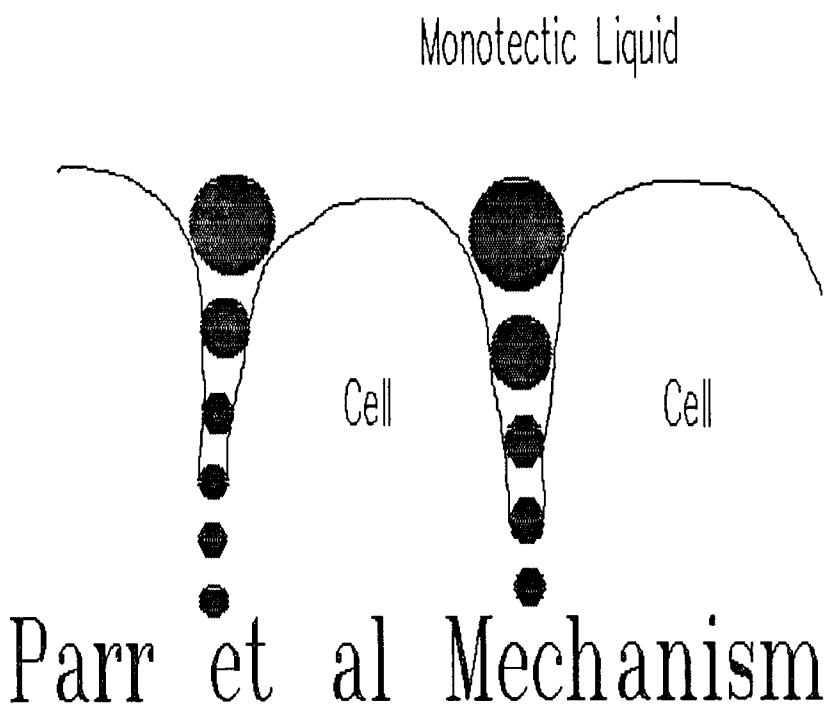

Figure 2. Schematic of the monotectic alignment mechanism proposed by Parr and Johnston.

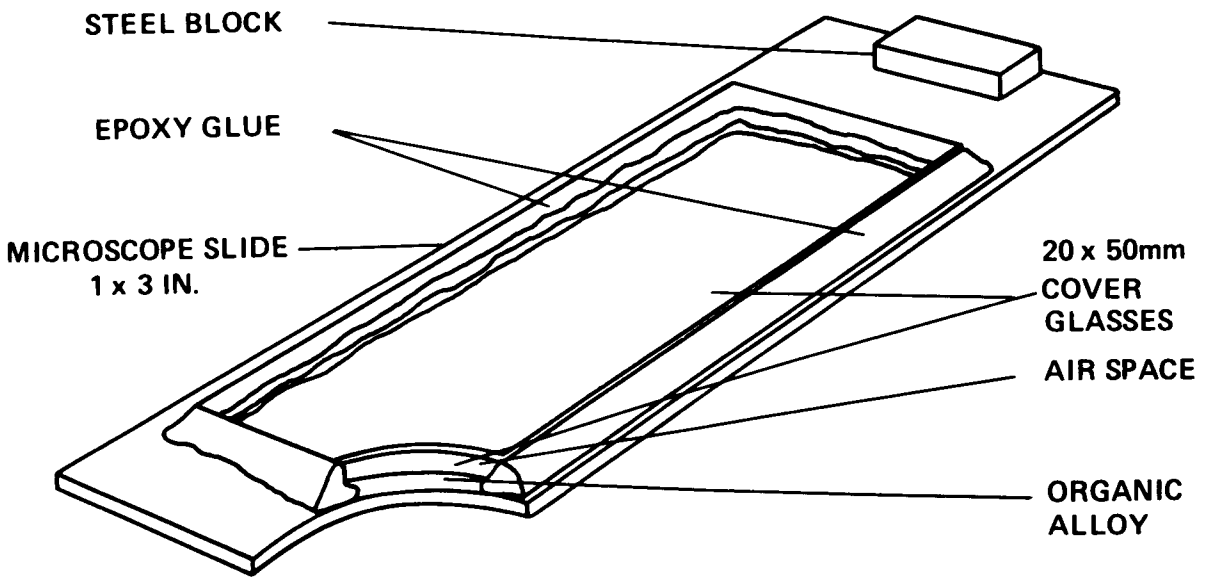

Figure 3. Sample cell for transparent alloy study.

slides across the two upper surfaces of the blocks and maintains contact on both ends. The blocks are independently temperature controlled to maintain a temperature gradient along the cell. The temperatures were selected so that the contents of the cell melted back from the hotter block until the solid-liquid interface was in the gap. The cell was illuminated through the gap and the interface was observed with a high magnification optical microscope. Photomicrographs recorded the interface morphology. Slowly pushing the cell across the blocks onto the cold block side caused unidirectional freezing of the melt. The cells were translated using a Burleigh Inch Worm (piezo-electric linear motor with precise positioning capability). Push rates of between 0.05 and 30 $\mu m\ s^{-1}$ were used. The apparatus is shown in Figure 4. More detailed descriptions can be found in the literature [7-9].

The thermal conductivity of the cell and the thermal transfer coefficient for heat transfer between the blocks and the cell determine the thermal gradient established along the length of the cell. The rate of pushing the cell can affect the gradient if the rate is higher compared to the thermal conduction through glass. A mock cell was constructed with a fine wire thermocouple embedded within an epoxy layer to simulate the organic specimen. Temperatures were plotted with time and position at translation rates similar to those used in the study. The thermal gradient in the cell was thus calibrated for the individual block temperatures. Only at growth rates much greater than those used in the study would the temperatures lag the push rate. Gradients could be obtained in the range from 8°C to 45°C cm^{-1}.

Specimens were placed on the stage and pushing of the cell (growth) was begun once the interface melted back to its equilibrium position. The interface reached steady state after a period of growth of 15 min to 1 hr. Sometimes changes in growth rate were intentionally made. The cell design gives a 1-cm-wide growth interface for observation. Several portions of the interface were photographed at 100X magnification. Multiple observations and measurements are possible.

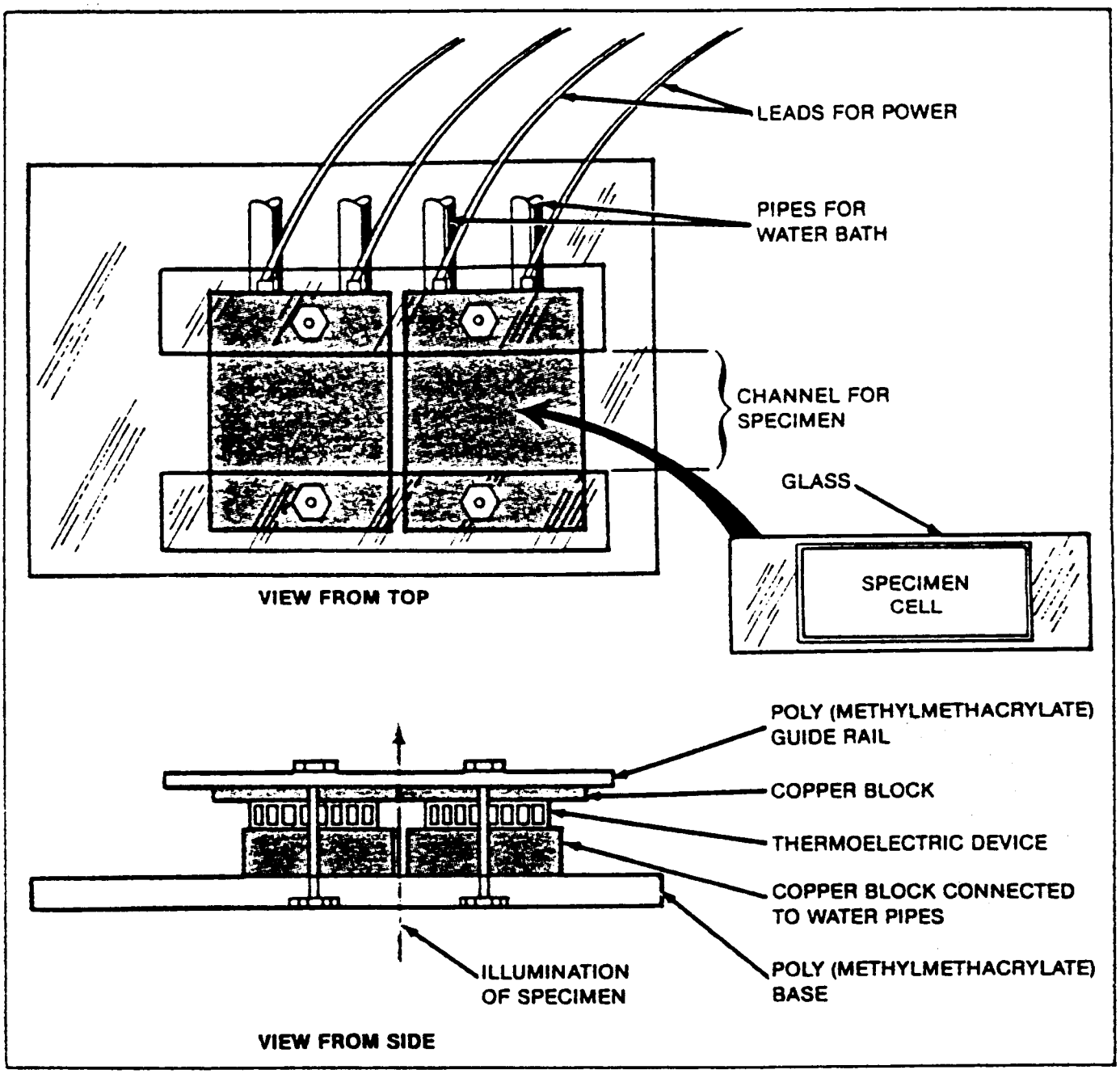

Figure 4. Apparatus for directional solidification and solid-liquid interface observation of transparent model material.

The organic materials must be in as pure a form as possible. The glycerol was spectrographic grade with less than 0.5 percent water. The water content of the starting material was checked using Karl-Fisher Titration. The succinonitrile was purified by performing fractional recrystallization from the melt using the apparatus schematically shown in Figure 5. The beaker of molten succinonitrile is stirred continuously to keep the heat flux in the liquid constant. As the cold-finger cools, crystallization of pure succinonitrile occurs on the finger surface. Impurities are rejected into the stirred melt. After one-fourth of the batch of succinonitrile is solidified, the finger

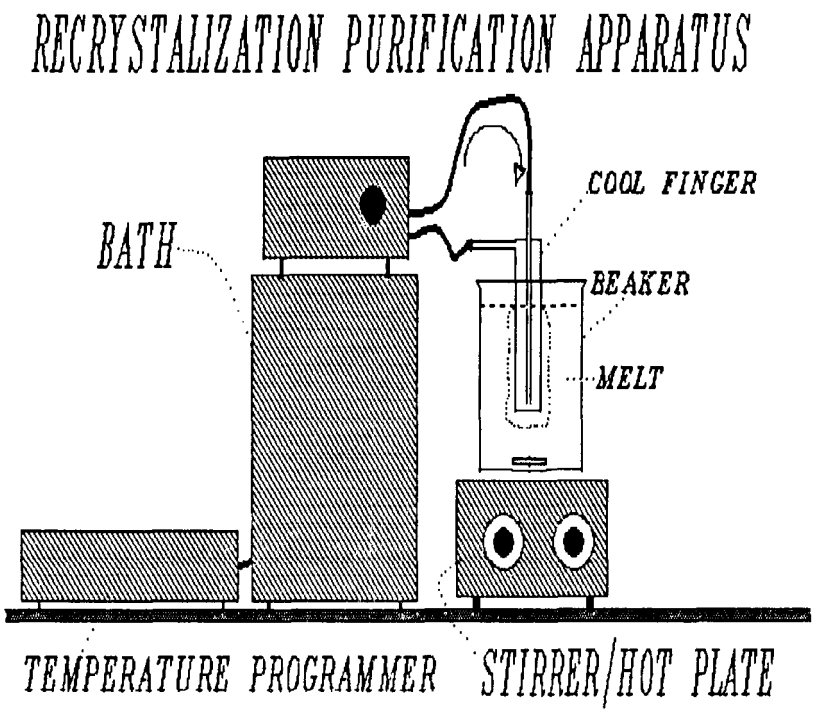

Figure 5. Apparatus for fractional recrystallization for purification of organic starting materials.

is withdrawn from the melt. Playing the hot air from a heat gun over the exposed surface forces the outer layer to melt off leaving a very pure batch of succinonitrile. After two recrystallizations, the succinonitrile was distilled to obtain the starting material. (The recrystallized material was not significantly improved by distillation but distillation under vacuum does remove the higher vapor pressure impurities.) Differential thermal analysis showed immeasurably negligible difference in purity after distillation from the zone-refined succinonitrile. The melting point data measured using the DTA apparatus was utilized for the phase diagram.

Upon mixing the two materials together, a slow degradation process began. The degradation is caused by the combination of heat and light on the solution. Procedures were therefore followed to make measurements with a minimum and consistent amount of handling. The solutions were prepared (in a dry atmosphere) and homogenized, and the cells were filled, sealed, and immediately put into a freezer — halting the degradation. If this precaution were not taken, in about two weeks at room temperature the solution would become discolored, which causes the solidification characteristics to change.

For phase diagram measurements, 75 ml of solution were needed to fill the specimen chamber of the apparatus shown schematically in Figure 6. Cloud point temperatures using a platinum resistance thermometer were found by measuring the scattering of laser light through the solution with a photodiode. The sharp voltage drop form the diode (scattering increased due to clouding) is the point when nucleation of second-phase liquid droplets occurs. Enthalpy release at this point is so minute that a change in the temperature trace is not practical to detect. (Some measurements were also made using a thermocouple with smaller volumes.) Rates of cooling were usually near 5° per hour. The melting curves were also taken, but as it is always the case, the

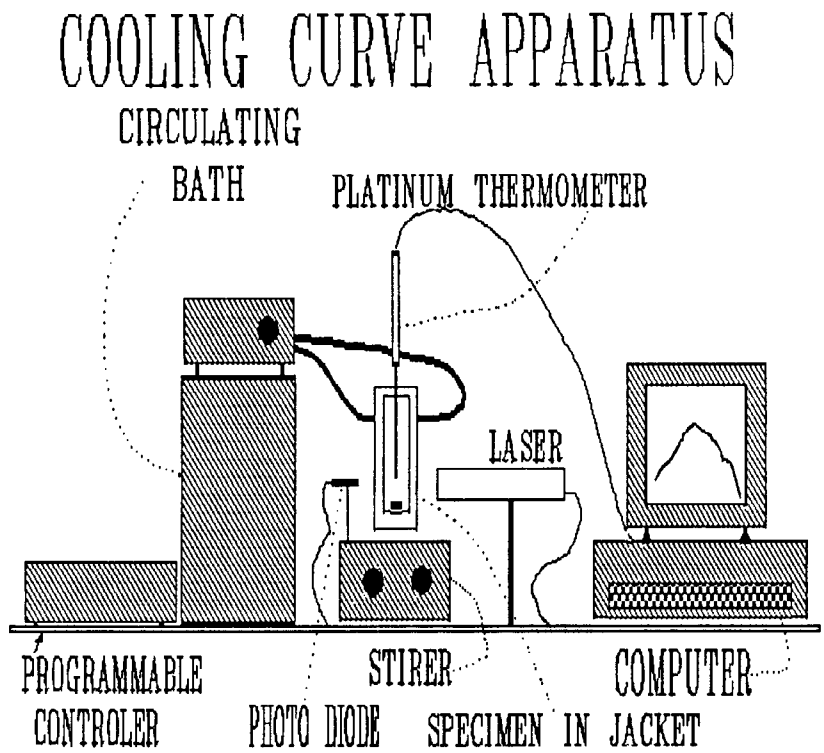

Figure 6. Apparatus for determination of phase diagrams of the transparent model monotectic alloy.

temperature inflection point at melting is not sharply defined. The platinum resistance thermometer used had an accuracy of better than 0.005°. The resistance thermometer and the light detector circuit data were collected by a micro-computer with IEEE-488 input. A computer program was written in IBM-PC compatible BASIC for this special data acquisition task and is included in the Appendix. A similar apparatus is described elsewhere [10].

Some measurements were made with the use of the Mattson Sirius 100 FTIR (Fourier transform infrared spectrometer). These measurements entailed performing repeated spectral transmission analysis on a series of points along the length of the specimen in order to determine the variations in composition caused by unidirectional solidification. A scan was made before and after unidirectional growth. Absorption peaks were selected to best obtain the glycerol concentration along the cell. Each measurement was done using the 100-μm-diameter aperture (representing the actual sampling area). The HgCdTe detector in the mid-IR was used. Scans starting from the quenched end of the specimen into the growth zone and on into the as-cast area were made with 25 to 50 points per inch. The spectral range was limited by the glass cell material (see results section). Although the organic layer was very thin, glycerol absorbs heavily on the 1 to 3 μm wavelength window. Thicker cells could be used only with less than 5 w% glycerol in succinonitrile.

THEORETICAL BACKGROUND

Considerable published materials for metal alloys are available for single phase planar, cellular, and dendritic, as well as eutectic, peretectic, and regular monotectic solidification [11-13].

Recent work with monotectic solidification using organic models is also available as a basis for analysis [14-16]. As far as we know, this work represents the first systematic research on cellular freezing of monotectics.

It is necessary to summarize solidification theories for simpler systems such as single phase types in order to appreciate the additional complexity of monotectic systems. Monotectic freezing is the reaction at the monotectic temperature and composition where $liquid_1$ forms two phases, a solid and another liquid, the $liquid_2$ phase. The phase diagram for this reaction is shown in Figure 7. "Regular" type monotectic growth results in a simultaneous formation of the second phases from the first liquid in a coupled manner. The phase diagram determines the amount of $liquid_2$ and solid that forms. Interfacial energies determine the arrangement of the phases in the casting [15]. During unidirectional growth, one arrangement could be a regular array of $liquid_2$ rods forming within the solid matrix normal to the solid-$liquid_1$ interface. The growth rate determines the rod spacing and diameter [11]. "Irregular" type growth results in a non-uniform arrangement of twisted strands that vary in cross section. For small volume fractions of $liquid_2$ it is possible to form a series of droplets. Interfacial tension arguments can be used to explain the rod structure instability [1,16]. Droplets can form either at the freezing front or shortly after (within the solid matrix) by Rayleigh instability.

Although the interface is polyphased, it can, as a first approximation, be treated as single phased for understanding constitutional undercooling that leads to cellular breakdown of the planar interface. Planar to cellular breakdown during eutectic solidification has been successfully modeled [11] for eutectics by assuming the two phases were so similar to each other that they could be considered as one phase. The same assumption could be applied to the monotectic interface to model constitutional undercooling.

Constitutional undercooling is a condition where the liquid ahead of the solid at the freezing front is enriched with solute to the point that the equilibrium freezing temperature of the liquid is below the true local temperature [13]. In this study, constitutional undercooling is induced by the excess solute creating a hypermonotectic solution. Growth at the monotectic composition will not result in constitutional undercooling (because this is an invariant point) and thus, all growth conditions result in planar type growth. For hypermonotectic solidification, the excess solute is rejected, builds up at the freezing front, and acts as an impurity. Depending on the growth rate and temperature gradient, the resulting constitutional undercooling can cause interfacial instability. The breakdown of the planar interface results in the formation of cells or dendrites. These cells or dendrites consist of polyphase monotectic. In the valleys between cell peaks, excess solute is trapped raising the average concentration of solute. Parr and Johnston's model suggests that the solute concentrations built up within these valleys cause droplets of $liquid_2$ to be deposited in the intercellular valley resulting in an aligned series of droplets.

For cellular breakdown to occur, hypermonotectic concentrations are not always required. Constitutional undercooling of the melt caused by a buildup of an impurity having a low distribution coefficient is more common. Moreover, the undercooling of the melt at the interface can be caused by both impurity addition and excess solute. Multiple impurities could each contribute to the constitutional undercooling. The effect is one of superposition and not synergistic.

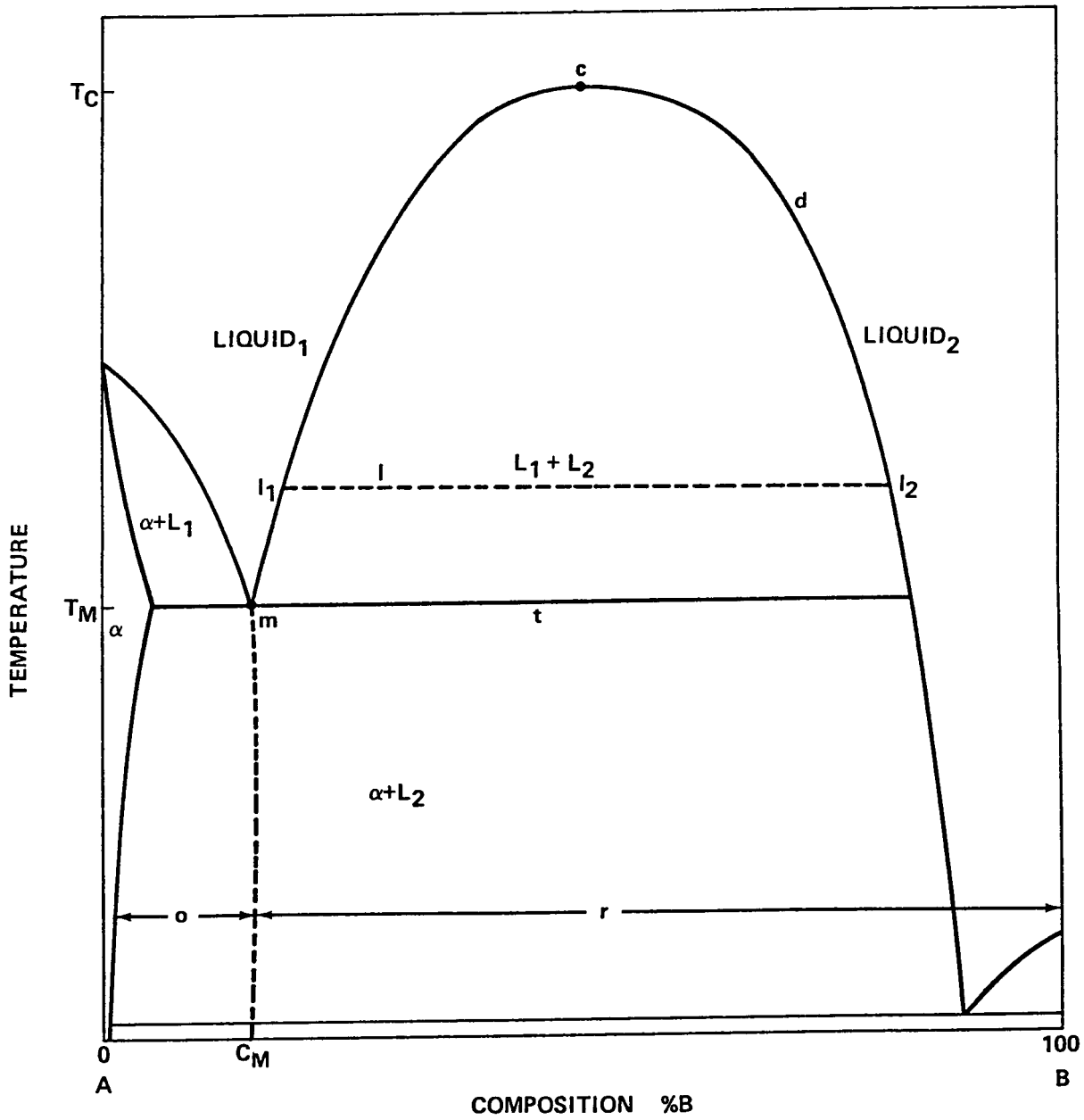

Figure 7. Monotectic alloy phase diagram.

Growth conditions and the interfacial properties of the system itself determine whether or not the liquid$_2$ droplets that form at the interface will be incorporated into the solid matrix. The alternative is that the liquid droplets will coalesce and be pushed along with the growth front until they grow to a size that forces incorporation by the freezing front by kinetic arguments.

For the succinonitrile-glycerol system, extra liquid$_2$ from solidification of hypermonotectic compositions was often incorporated into the solid matrix at the freezing front resulting in a higher volume fraction of that phase. Smooth, planar interfaces could be grown this way.

For a first approximation, solute effects at the interface can be modeled with the single phase model of Burton, Primm, and Schlichter (BPS) equations [11,17]. It differs from equations by Tiller et al. [13] in that a characteristic boundary layer is assumed and an effective distribution coefficient is defined.

The composition within the fluid at a point x away from the solid is

$$C(x) = C_\infty \quad \frac{k_o(d_F/d_s) + (1 - k_o d_F/d_s)\exp(-xV_s/D)}{k_o(d_F/d_s) + (1 - k_o d_F/d_s)\exp(-\delta V_s/D)} \tag{1}$$

where d is density referring to fluid and solid phases, δ is the boundary layer thickness, k_o the equilibrium distribution coefficient, V_s the solidification velocity, D the diffusion coefficient, and C_∞ the composition of the fluid well away from the interface. This equation models the segregation of solute at the moving interface and includes the density change from freezing. Using a "boundary layer thickness," an effective distribution coefficient was defined

$$k = k_o/[k_o + (1 - k_o)\exp(-V_s\delta/D)] \tag{2}$$

where for simplicity, the densities of the solid and liquid were set equal. Solute transfer inside the boundary layer is by diffusion only. Solute transfer outside the boundary layer is by convection. An estimate of the boundary layer thickness can be made from

$$\delta \approx D/V_s \quad . \tag{3}$$

From these equations, calculations of the solute concentration can be estimated, or alternatively, the boundary layer thickness, the effective k, or the diffusion coefficient could be empirically measured. Figure 8 schematically shows the solute concentration distributed along a unidirectionally solidified specimen. The diagram shows the result of having convection within the specimen during growth. Convection distorts the solute build up at the interface and alters the characteristic concentration profile. For the growth conditions of this experiment, where cell gaps are in the tens of microns range, the assumption of strict diffusion control is a very good one.

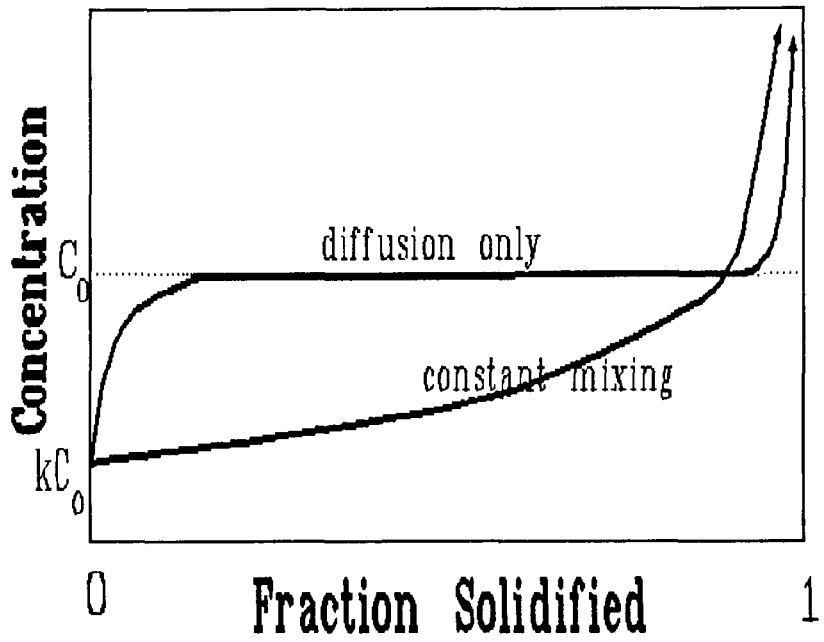

Figure 8. Schematic of solute distribution during solidification for alloy with and without convective mixing.

EXPERIMENTAL RESULTS

In brief, the phase diagram of the system was re-evaluated, a stability diagram assembled showing conditions for cellular breakdown, cell size measurements summarized, and measurements of the apparent concentration variation along the unidirectionally grown specimen made by FTIR analysis.

A. Phase Diagram

The succinonitrile-glycerol phase diagram, as amended, is given in Figure 9. The best estimates of the monotectic composition and temperature are 8.22 w% and 47.4°C. All changes from the previous data (Grugel and Hellawell [16]) tend to raise the tie lines and shift the monotectic composition to the right. This can only be attributed to using starting materials with higher purity. A very small (0.2°) difference exists between the literature value for highly zone refined succinonitrile and that from this work. (Instrument error in the apparatus for determining the cooling curves may account for some of this difference since the large platinum resistance sensor could be reading a lower temperature due to cooling from the surroundings.) Cooling rates of 5° per hour were used for these measurements. This provides a reasonable approximation to equilibrium conditions. Upon reheating and cooling again, the solutions showed marked depression of both cloud point and monotectic isotherm. The first measurement was therefore the most accurate (free from degradation products). Figure 10 is a plot of the cooling curve and cloud point determination for one run. Appendix B shows all the data points.

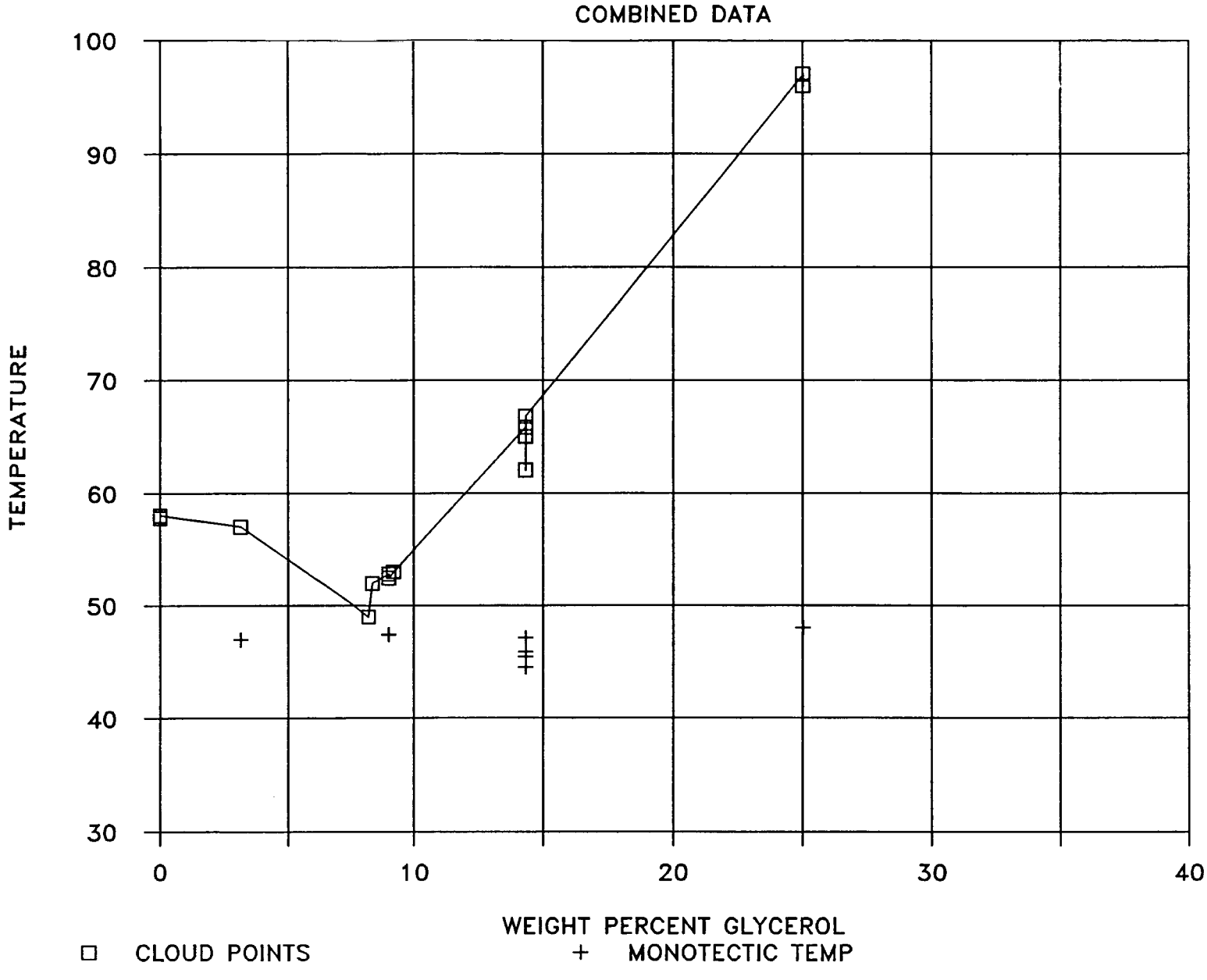

Figure 9. Phase diagram data for succinonitrile-glycerol.

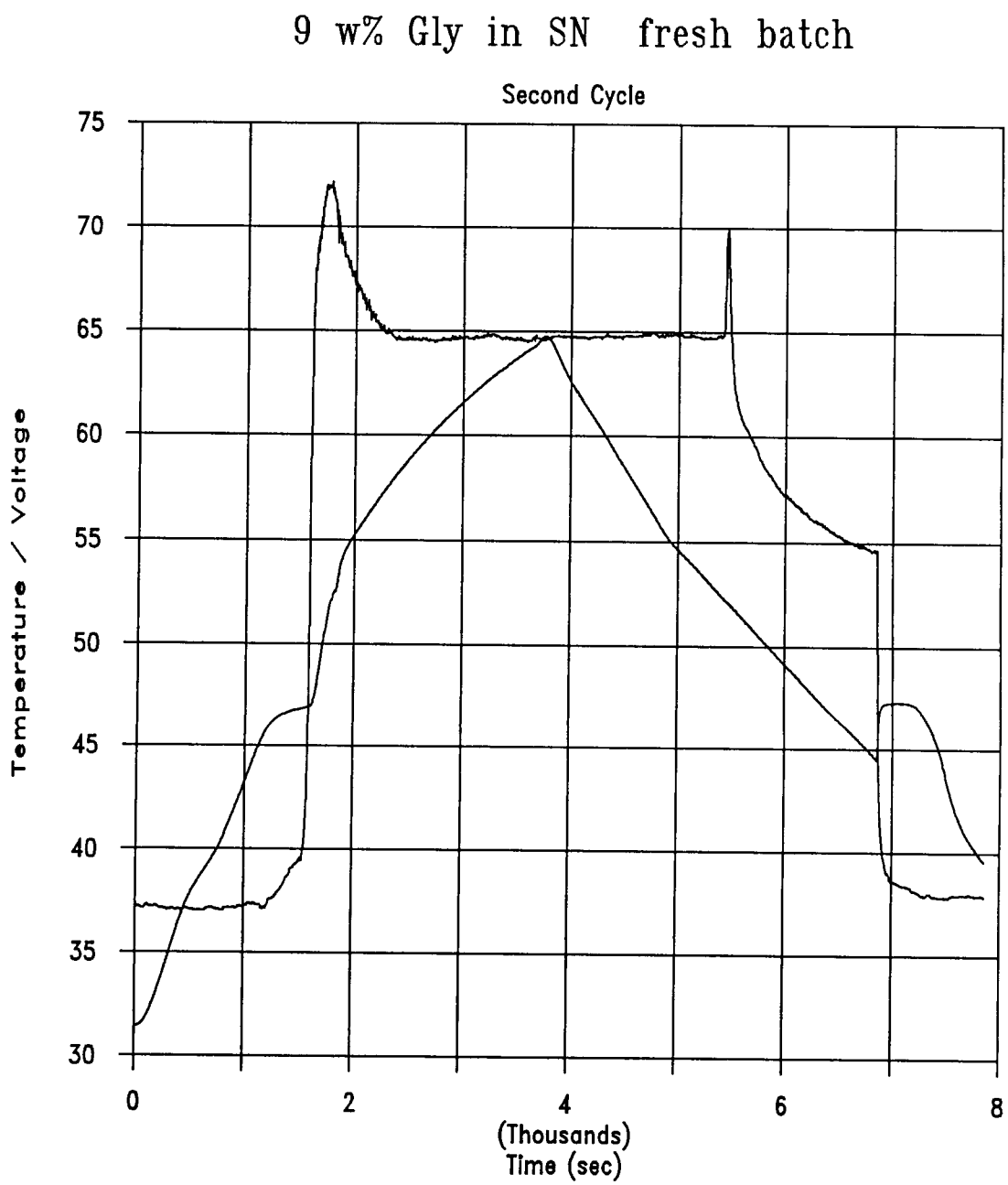

Figure 10. Sample cooling curve for succinonitrile-glycerol.
Upper curve – photo-detector voltage,
lower curve – temperature °C.

B. Stability Diagram

Figure 11 is a stability diagram determined for the system. The observed interface morphology is mapped over the domain of growth condition (G/R) and composition (8 to 16 w% glycerol). The separation between cellular and planar growth is clear. The theoretical boundary curve included is based on a single phase alloy model of the monotectic [equations (1) to (4)]. Solute concentration above the monotectic requires a higher G/R (higher thermal gradient or lower

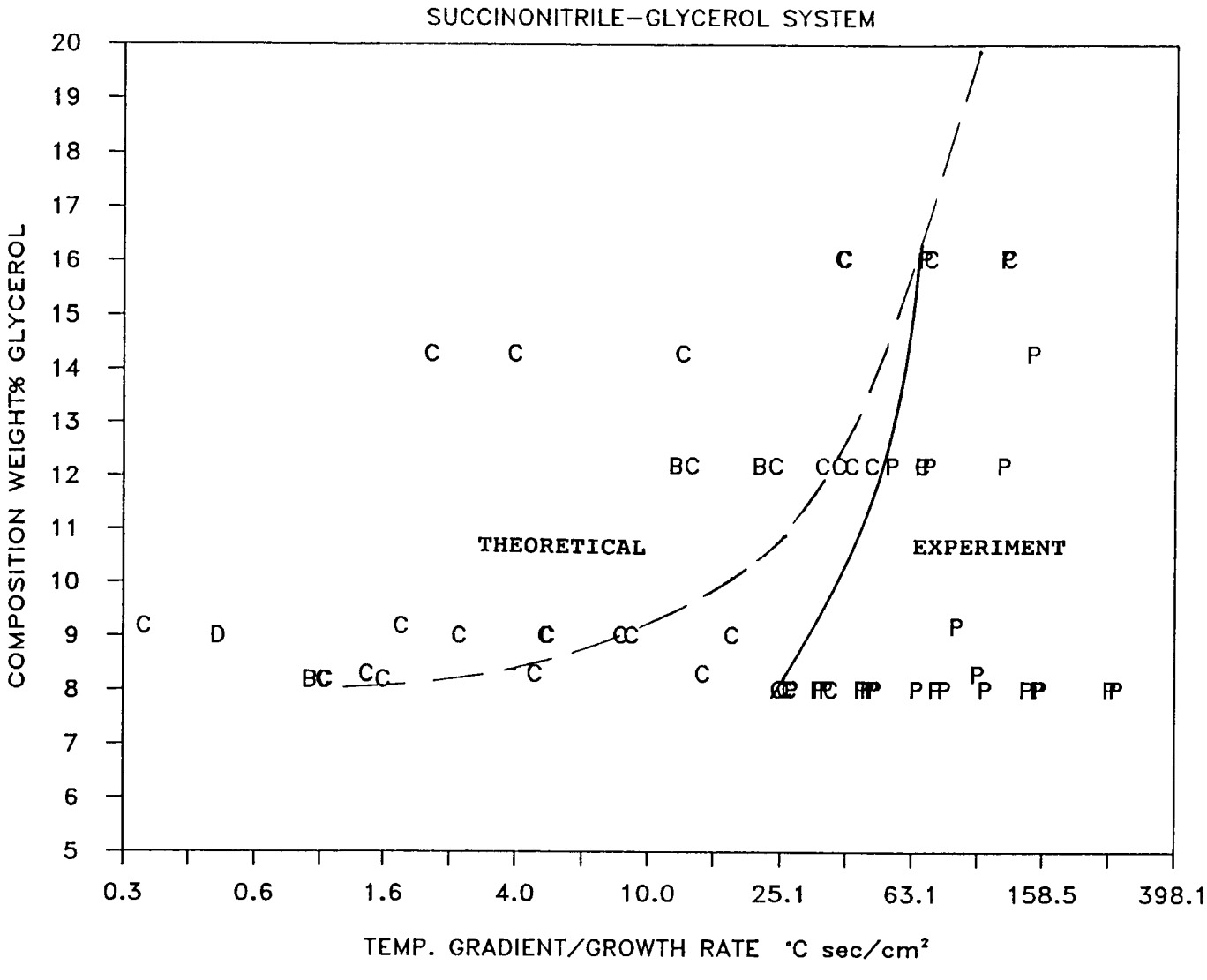

Figure 11. Stability diagram determined for planar, cellular, and dendritic growth.
Dashed line is the theoretical curve for planar stability.
Solid line is based on experimental observation.

growth rate) in order to maintain planar growth. Planar growth at the minimum G/R determines the edge of stability for planar growth. Data points for dendritic breakdown and branched cells are also shown. Appendix C shows all the data for the diagram.

C. Stability Theory

Based on the BCS model, planar growth of on-monotectic should be possible for all ranges of G and R. This would put the end point of the breakdown boundary at G/R = 0 and 8.2 w%. However, because the materials are not 100 percent pure, a constant shift to the right is seen experimentally. This shift represents the accumulated effect of the impurities. As long as the same purity levels and handling procedures are followed, this shift is a constant for all measurements. The major impurity is the trace quantity of water that was introduced with the glycerol and is very difficult to remove. Water has a very low solubility in succinonitrile and is therefore rejected at the solidification front.

The condition of breakdown follows from the Tiller et al. [13] paper is described thus:

For stable (planar) interfaces,

$$G/R \geq -m(C_o - C_m)/D \tag{4}$$

where m is the slope of the liquidus (in this case of the monotectic dome) on the phase diagram, C_o the solution concentration, and C_m the monotectic composition. This inequality is nearly identical to the single phase case. Here, as one deviates from the monotectic composition, the solute buildup (not cleared by diffusion) can lead to constitutional undercooling. Equation (4) was written for the hypermonotectic case. The difference in C would be opposite in sign for hypomonotectic solutions. A difficulty in interpreting this type of equation is in the definition of m. There is no liquidus on the hypermonotectic side of the diagram. The thermodynamic argument for the use of the local slope of the immiscibility dome is that the behavior of the chemical potential (free energy of the three phases versus composition) of the two components mimics a eutectic phase diagram. This is shown schematically in Figure 12. In other words, the monotectic reaction represents the case of increased non-ideality from the eutectic case. (Hidden within every eutectic is a monotectic.) Another view is that the second phase is merely liquid instead of solid as in the eutectic case.

To calculate the theoretical curve in the stability diagram (Fig. 12), D was set to 3.5×10^{-5} cm^2 s^{-1} and m to 2.8. The value of D for succinonitrile melt is from the literature [15,18], as no measure of its value was made. The slope of the dome at the monotectic composition taken from the phase diagram gives the value of m.

Sometimes a cellular growth datum point can be found to the right of the boundary on the stability diagram (Fig. 11). After prolonged growth, impurities collect at the interface and promote cellular breakdown at a growth rate which has already been shown to maintain planar growth. Planar growth can be reinstated with an appropriate reduction in speed. For most of the points in

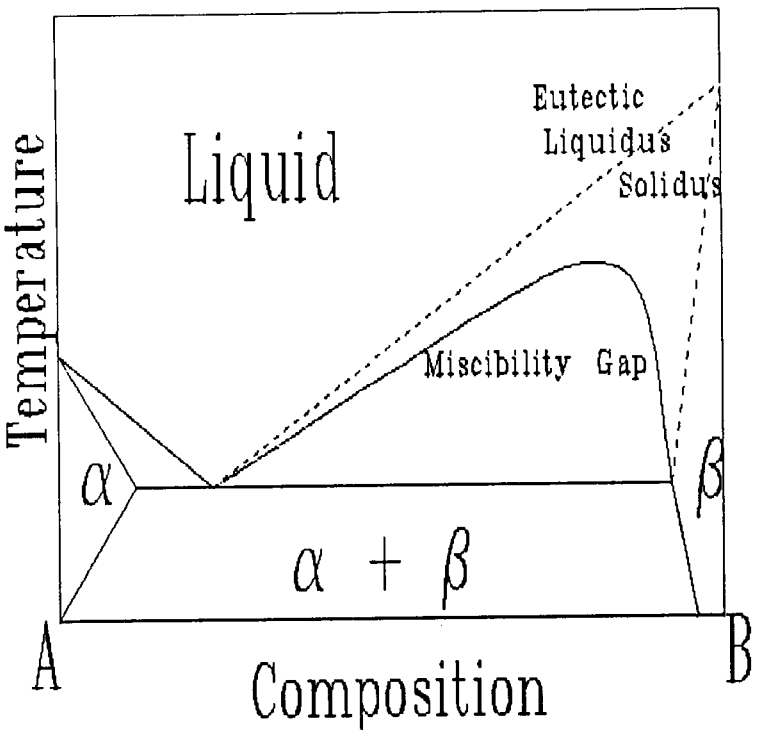

Figure 12. Extension of monotectic phase diagram to eutectic type phase diagram.

the stability diagram, the observed morphology was noted once steady state was reached. Solidification would be allowed to proceed for approximately a half hour to ensure steady state conditions were reached. Steady state growth is reached after the initial transient (as in Fig. 8). For the conditions of $D \approx 2 \times 10^{-5}$ cm^2 s^{-1} and rates near 2×10^{-4} cm s^{-1}, steady state is reached in 0.1 cm of growth, or at that velocity, within a quarter of an hour [see equation (3)]. It is worthwhile noting that other organic systems solidified under similar growth conditions have similar boundary layer thicknesses. Some experimentally measured values are as follows [17]:

TABLE 1. EXPERIMENTAL BOUNDARY LAYER VALUES

System	δ (cm)
10 Percent Benzoic Acid in Napthalene	0.07
0.2 g/100 ml Urea in Water	0.02
0.1 Percent Tetracene in Anthracene	0.20

D. Solute Concentration Profiles

Some preliminary measurements of solute profile were made using the FTIR. A technique was developed for determining the glycerol concentration variations within the cell after unidirectional growth. The FTIR permitted repeated measurement of the IR transmittance in a 100-μm spot through the cell. This was done at uniform intervals along the sample length. Figure 13 shows a set of spectra from the FTIR. The four spectra include the pure succinonitrile (Fig. 13a), the pure glycerol (Fig. 13b), the glass of the cell (Fig. 13c), and a 12 percent glycerol alloy (Fig. 13e). The glass spectrum for a cell was subtracted from all spectra. Also shown is the transmittance "window" through which the organic spectra could be detected. The path length of the organic was approximately 10 to 30 μm. Glycerol absorbs so well that even this thin layer caused 100 percent absorption for some of the measurement conditions selected. The monotectic solutions measured had only between 8 and 16 w% glycerol.

One scan line of points is 2.5 cm long. For the two sets of curves shown in Figures 14 to 16, either 25 or 50 individual spectra were taken at uniform intervals along this line. The scan line traversed the specimen from the quenched end, through the unidirectional growth zone and into the as-cast region which was never melted once the cell was filled. From each spectrum, the peak height at 3359 and at 3096 wave numbers was taken, which is a peak absorbence for glycerol and for succinonitrile, respectively. From the height at each measurement point of the glycerol contribution to absorption, a graph can be made to reproduce the variation of glycerol concentration (Figs. 14 and 15).

Systematic errors and noise were reduced by making two scans (Fig. 16). An initial scan of the solid sample prior to performing unidirectional growth was then subtracted from the scan after growth to remove specimen irregularities and machine error. The improvement can readily be seen when comparing Figures 14 and 16.

Two significant observations can be made from the scanned data. The first is that the initial transient for growth is readily observed as a sharp change in slope of the variation of absorbence as a function of location of the specimen. The transient is not as severe for the near monotectic composition (8 w%). The second observation is the evidence that the rejected solute concentration profile was quenched into the specimen. Considerable refinement of the method is possible. These improvements will produce greater spatial resolution and establish standards for quantitative analysis. Precise quantitative analysis cannot be performed at this time because each cell has different characteristics (e.g., thickness). A precise standardization of each specimen would allow for cell-to-cell variations.

In the 16 w% scans, midway in the growth zone is a perturbation which is directly attributable to a step change of growth rate. Sensitivity to growth conditions like this encourages use of this method to analyze solidification behavior. One comparison that is needed is to determine the degree of solute incorporation caused by cellular freezing condition versus planar solidification.

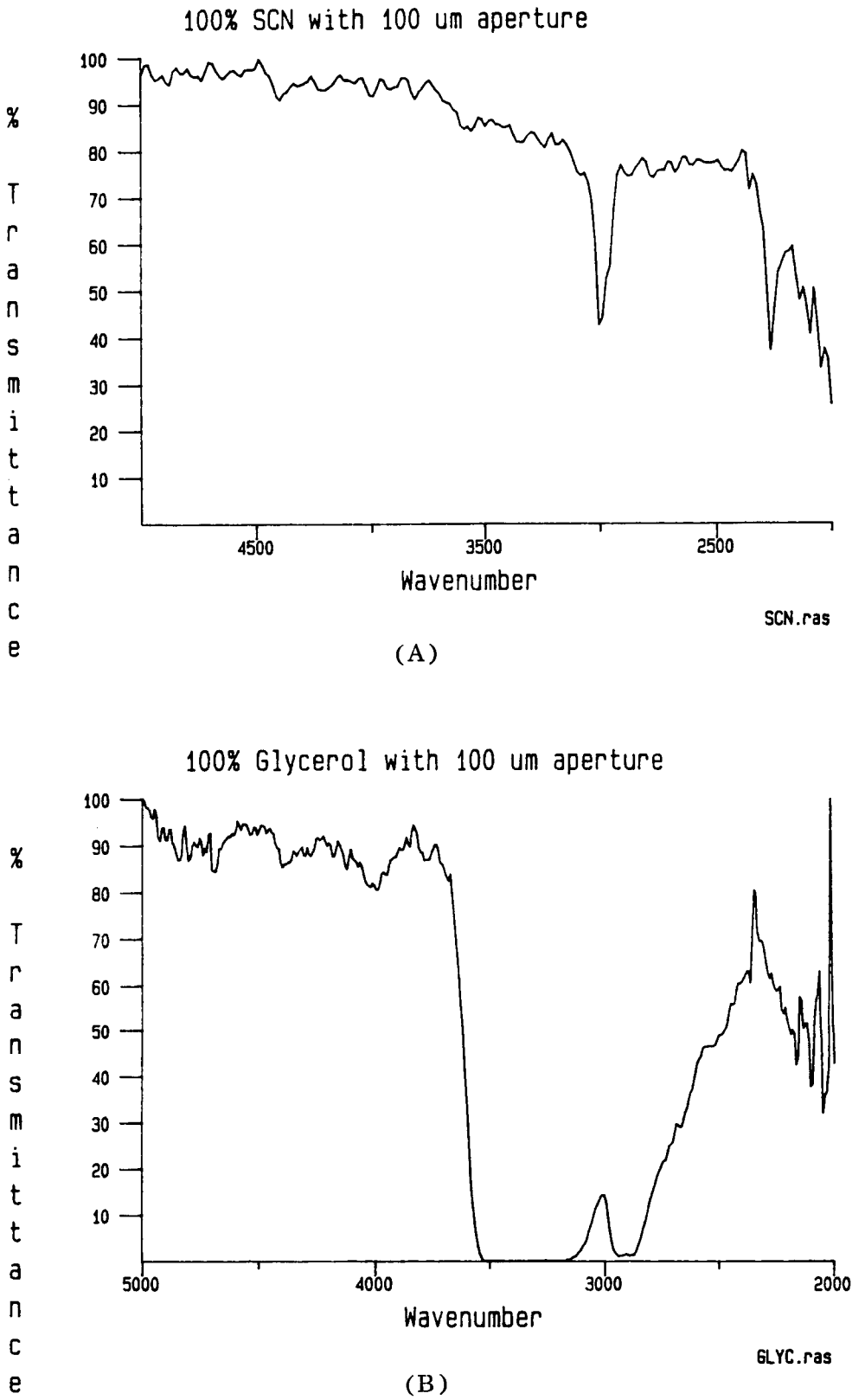

Figure 13. Sample FTIR scans: (a) 100 percent SN, (b) 100 percent glycerol, (c) glass sample cell, (d) 12 percent glycerol-SN transparent alloy.

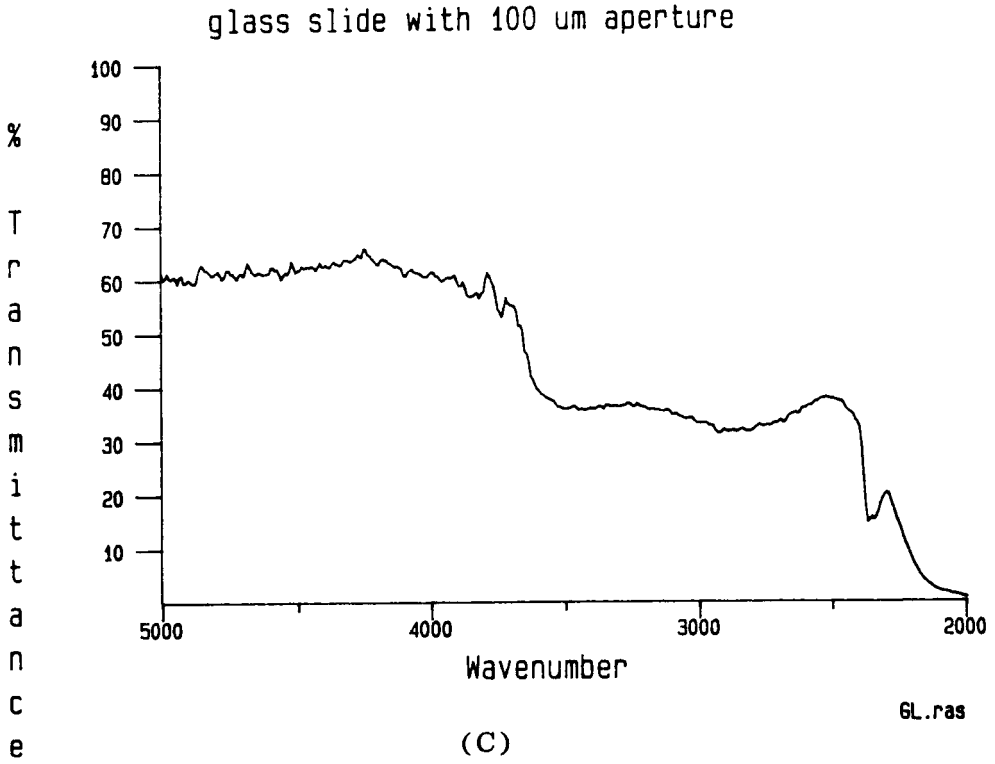
glass slide with 100 um aperture
% Transmittance
100
90
80
70
60
50
40
30
20
10
5000
4000
3000
2000
Wavenumber
GL.ras

(C)

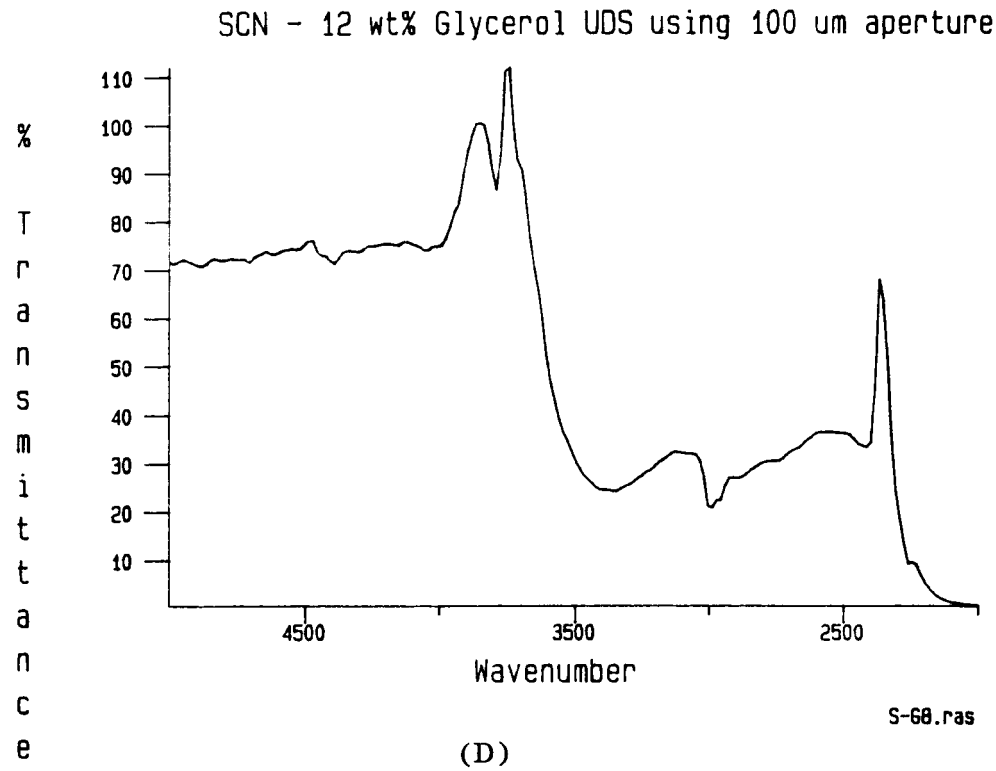
SCN - 12 wt% Glycerol UDS using 100 um aperture
% Transmittance
110
100
90
80
70
60
50
40
30
20
10
4500
3500
2500
Wavenumber
S-68.ras

(D)

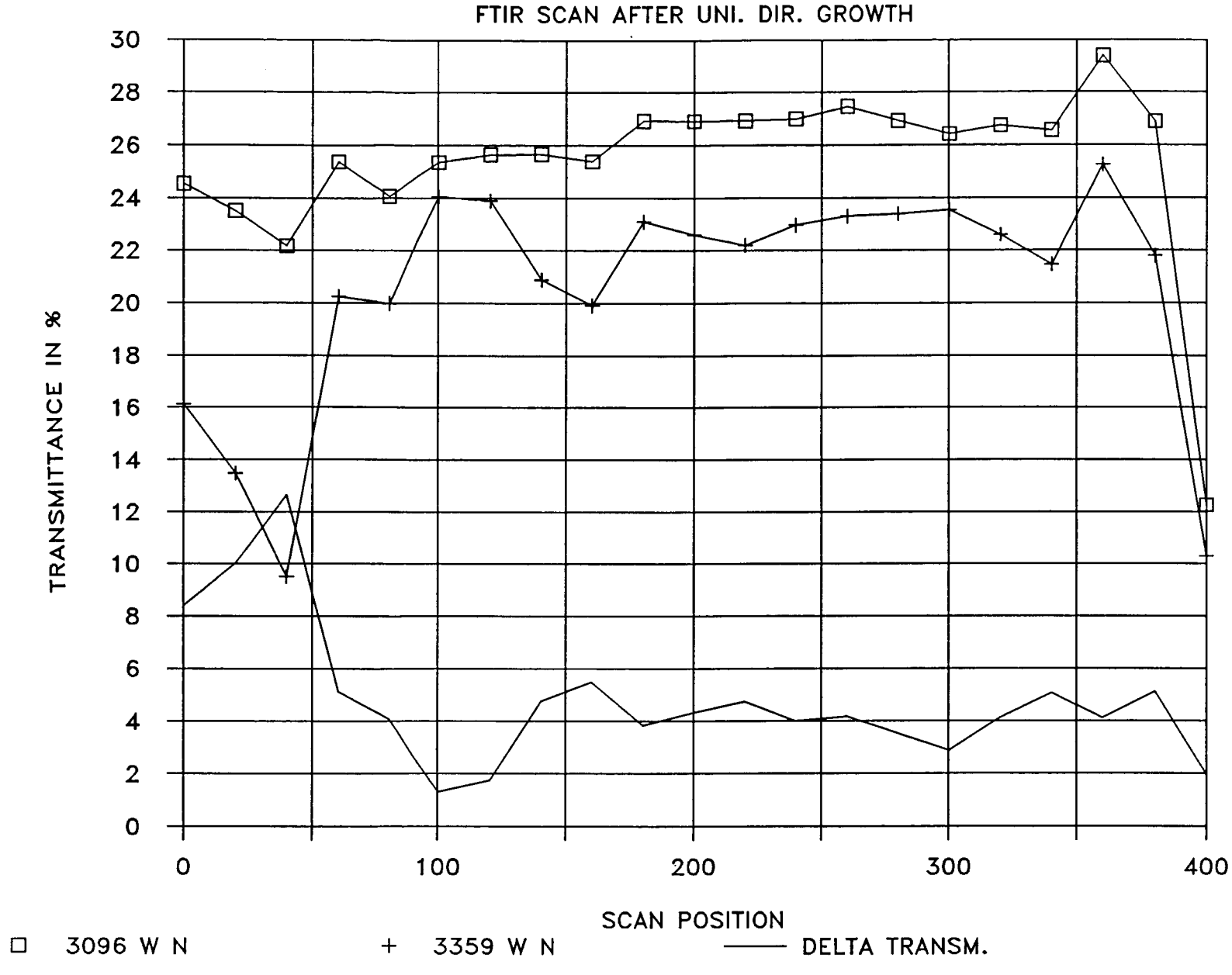

Figure 14. FTIR scan of 8 percent glycerol sample after unidirectional solidification experiment. Quench zone 0-50, UDG zone 50-120, as cast 120-400.

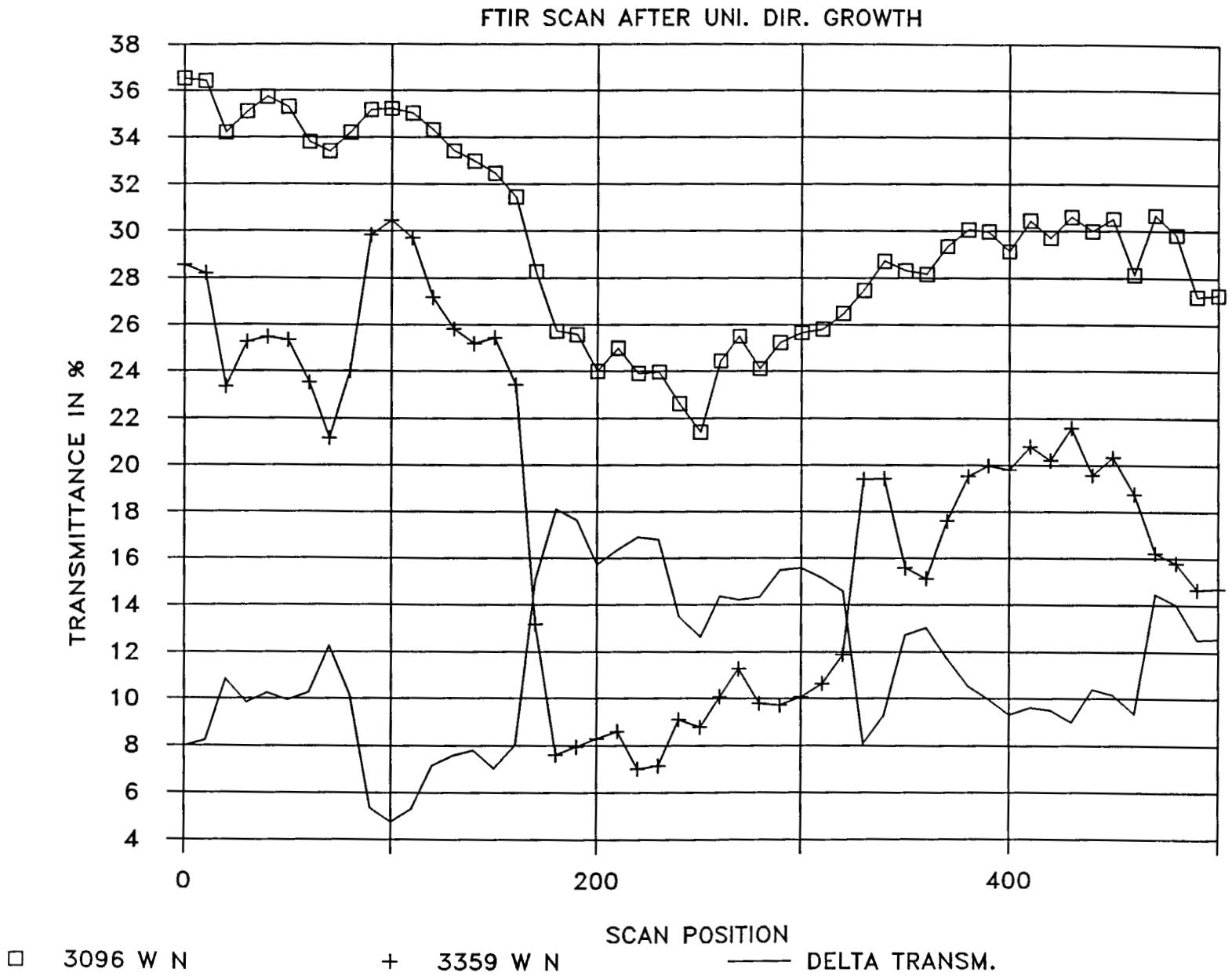

Figure 15. FTIR scan of 16 percent glycerol sample after unidirectional solidification experiment. Quench zone 0-70, UDG zone 70-180, as cast 180-500.

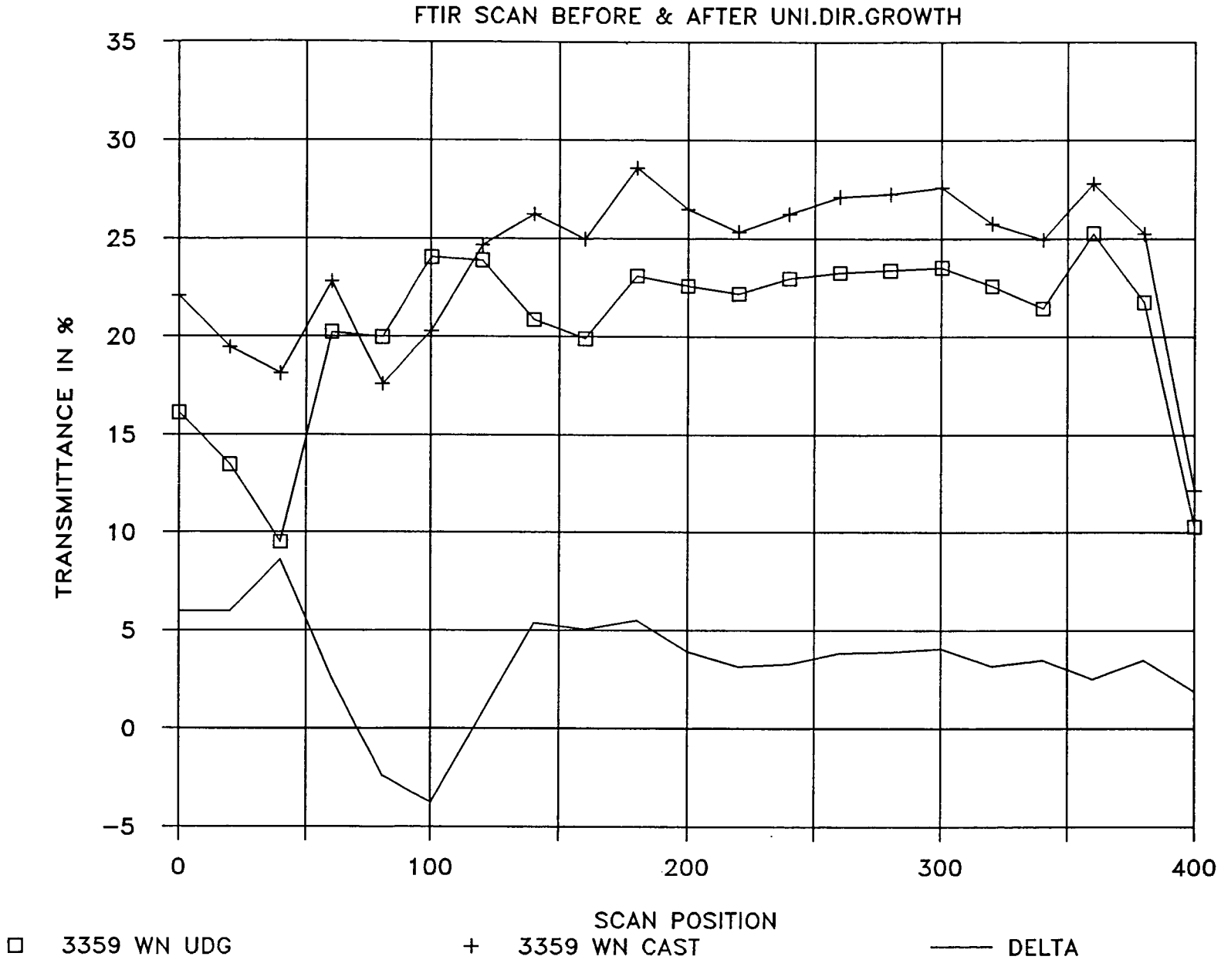

Figure 16. FTIR scan of 8 percent glycerol sample after unidirectional solidification experiment. Quench zone 0-50, UDG zone 50-120, as cast 120-400.

E. Intercellular Spacing

From the micrographs taken of the growing cellular interfaces, cell widths were measured using a graphics tablet and computer. A computer program was written for this task. A copy of the listing is in Appendix D. Figure 17 is the complete set of cell spacing measurements. Cell width is plotted against the $(GR)^{-1}$ at growth. $(GR)^{-1}$ is used for the abscissa because of the theoretical dependence of cell volume on the growth rate and gradient. Usually, the relationship results in a monotonic increase in cell width with $(GR)^{-1}$. A wide range of growth conditions will not usually produce a very large range of cell widths [11]. The limited composition range and large degree of scatter in the cell size data in Figure 17 do not allow determination of the cell size versus $(GR)^{-1}$ slope for our system without further study.

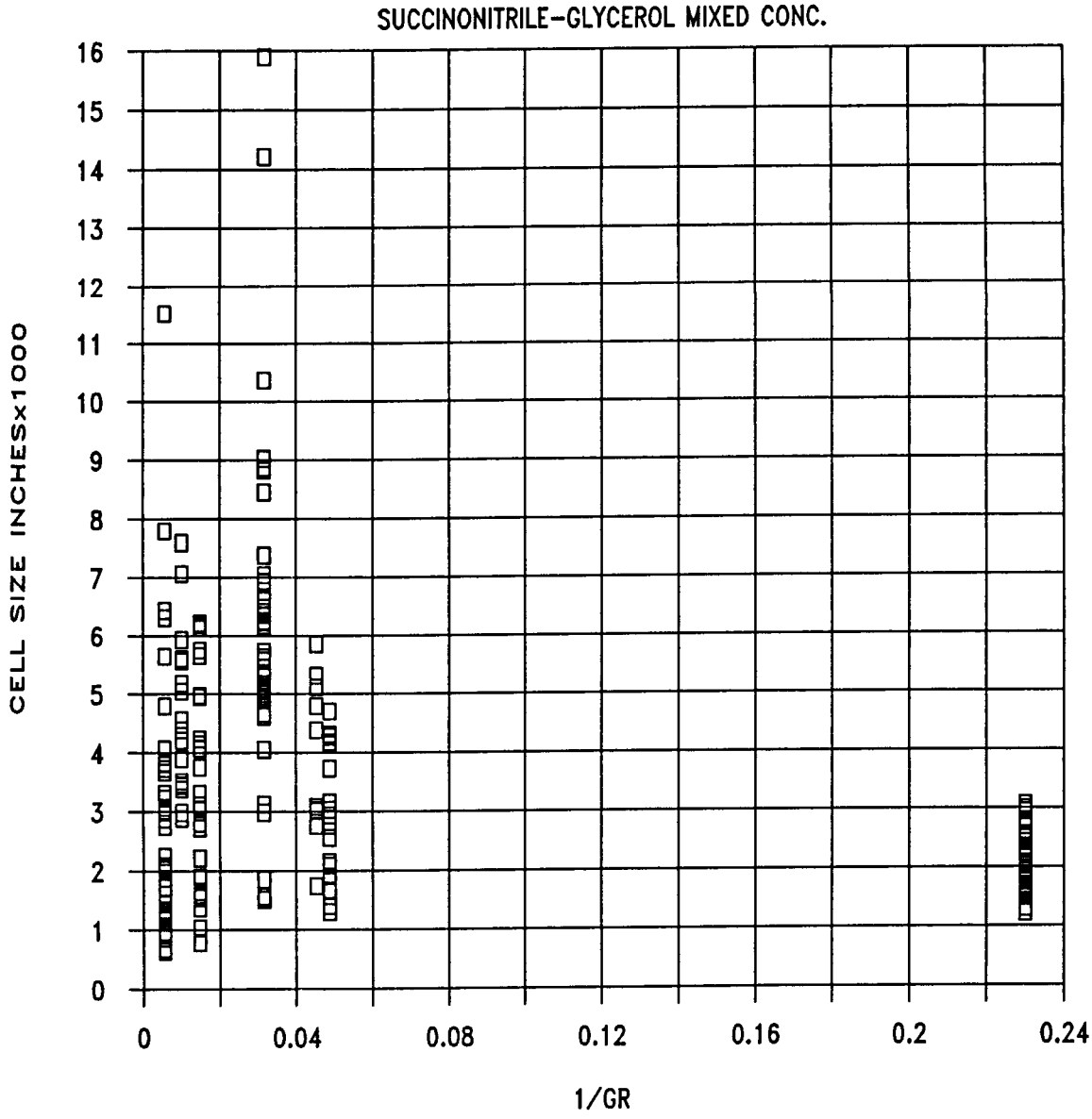

Figure 17. Cell size versus 1/GR for succinonitrile-glycerol alloys of various compositions.

F. Experimental Observations of Phase Alignment

This transparent system was selected specifically to allow the observation of the interface morphology during growth. This allows experimental verification of alignment mechanisms during planar and cellular growth. Conditions were generated to test the theories. Particle alignment has already been shown to occur in similar organic systems [15,16] during planar growth, but, cellular breakdown of the monotectic interface was never addressed. The Parr and Johnston model was determined from examination of metal alloy castings. To test the PARR and Johnston model, direct observation of cellular monotectic interfaces is required. The use of hypermonotectic compositions provides the excess solute to promote constitutional undercooling and breakdown of the interface. The volume fraction of liquid$_2$ phase is increased so that droplets of this phase may be deposited in the cell boundaries.

During planar growth, the alignment of second phase is generally observed. Under some conditions, regular arrays of particles are formed (Fig. 18) or liquid rods (Fig. 19). These results reproduce the data of Grugle and Hellawell. Under some solidification conditions of irregular-shaped rods formed (Fig. 20). Planar growth with hypermonotectic compositions often resulted in the excess liquid$_2$ collecting in larger diameter rods at regular intervals with smaller rods of liquid$_2$ in between. This was also observed within large (interface) cells. The intervals between larger rods were of the order of cell spacings and may be the precursors to cell boundaries.

It was possible sometimes to see the liquid$_1$-liquid$_2$ interface at the ends of the embedded rods of liquid$_2$ as a hemispherical cap which protrudes a little ahead of the solid-liquid$_1$ interface. The liquid caps accumulate excess liquid$_2$ droplets (that may have been on the glass surface) during growth.

The mechanism for particle alignment described by Schaefer et al. [4] (droplet trapping between the cell walls with subsequent Rayleigh instability breakdown from rods to spheres) was not observed. It was observed that cellular growth did promote the collection of excess solute in the intercellular regions. An increased volume of liquid$_2$ particles was observed in the cell boundaries after the interface passed. It is this liquid which would subsequently be trapped in the cell boundary. Aligned strips of liquid$_2$ particles form at the cell boundaries. However, this was always accompanied by intracell alignment (Fig. 21). Parr and Johnston [3] interpreted Al-Bi microstructures by suggesting that the spacing between liquid$_2$ droplets was of the order of the cell size. This did not occur, under the growth conditions of this study, in the transparent system.

A second prediction of the Schaefer et al. model is that the cell boundary cusp depth would be directly related to the instability leading to spherical droplet formation from rods. Rods are favored for shallow cusps. Deep cell cusps cause the Rayleigh-type instability and subsequent rod breakdown to aligned spheres. In the observations of the organic solutions, a wide range of cusp depths were established. No systematic pattern was seen for the formation of spheres based upon cell cusp depth. Both rods and particles of liquid$_2$ would form in the intercellular regions. Thus, our data do not support an intercellular alignment mechanism based on a Rayleigh breakdown.

Figure 18. Micrograph of planar interface SN-glycerol alloy showing aligned spheres. 200X

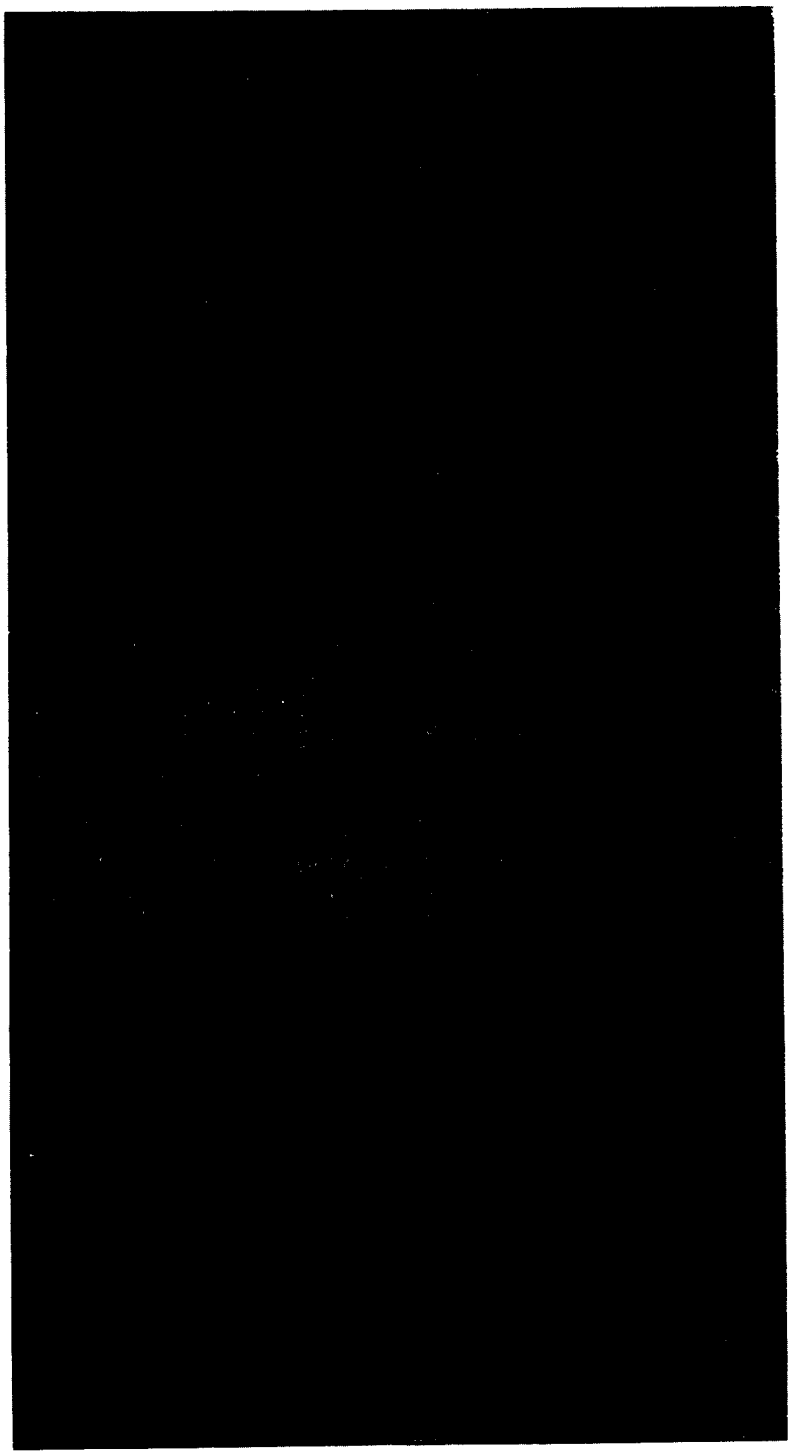

Figure 19. Micrograph of planar interface SN-glycerol alloy showing aligned rods. 200X

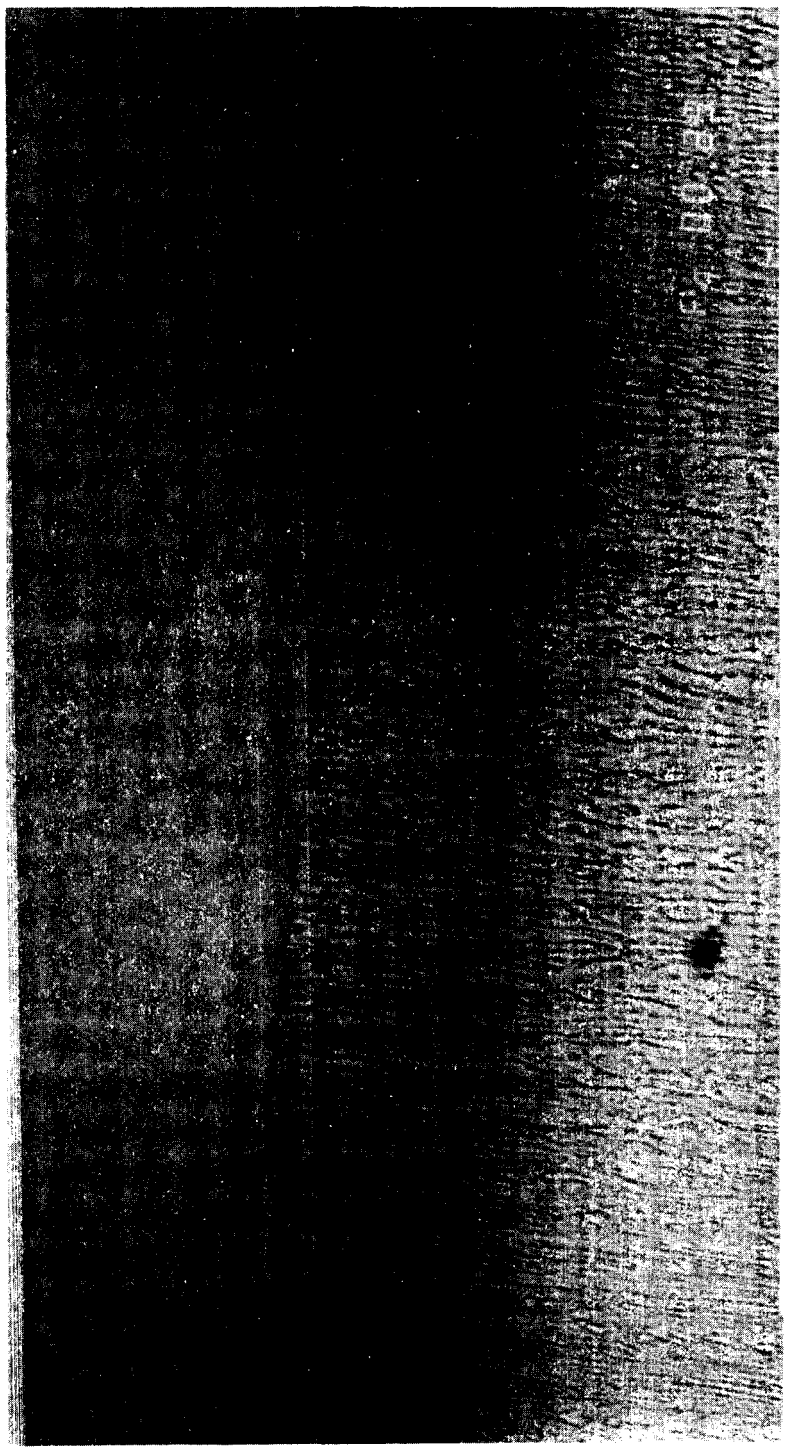

Figure 20. Micrograph of planar interface SN-glycerol alloy showing irregular rods. 200X

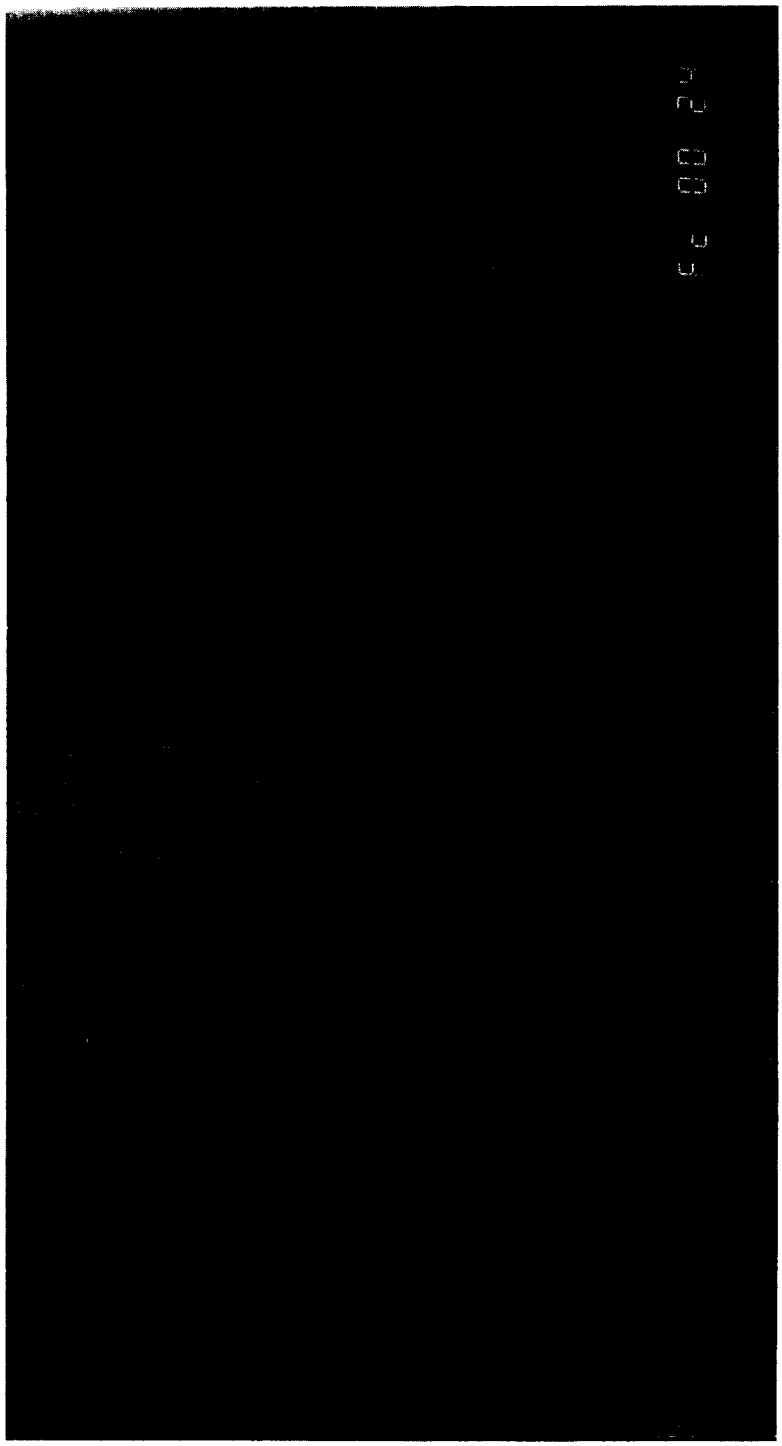

Figure 21. Micrograph of cellular interface SN-glycerol alloy. 200X

SUMMARY AND CONCLUSIONS

1. Cellular growth of succinonitrile-glycerol, SN-G, monotectic transparent alloy system has been systematically studied for 8, 12, and 16 percent compositions.

2. The SN-G phase diagram has been determined at compositions near the monotectic composition.

3. The region of stability, stability diagram, for SN-G has been determined for planar growth as a function of growth parameters and composition and compared to BPS theory.

4. Fourier transform infrared spectroscopy, FTIR, was utilized to measure solute segregation during growth. Further development of the technique could enable quantitative tests of solidification theory.

5. Monotectic second-phase alignment was observed to occur during planar and cellular growth. The second-phase spacing was always smaller than the cell spacing. Cell cusps produce second-phase rods of larger diameter interspaced within intracellular rods. Rayleigh breakdown of second-phase particles in the cell cusps was not observed.

15. Grugel, R., Lograsso, T. A., and Hellawell, A.: The Solidification of Monotectic Alloys – Microstructures and Phase Spacings. Presented TMS/AIME Fall Meeting, Atlanta, GA, 1984; submitted to Met. Trans. A.

16. Grugel, R. N., and Hellawell, A.: Monotectic Alloy Solidification-Determination of the Liquidus Surface in the System Succinonitrile-Ethanol-Glycerol. Mat. Res. Soc. Symp. Proc., Vol. 19, Elsevier Science Publishing Co., Inc., 1983, pp. 417-422.

17. Rosenberger, F.: *Fundamentals of Crystal Growth*. Springer-Verlag, New York.

18. Schaefer, R. J., Coriell, S. R., Rehm, R. G., and McFadden, G. B.: Convection During Unidirectional Solidification. NBS Report, NBSIR 82-2560, Materials Measurements, July 1982, p. 39.

APPENDIX A

PROGRAM CODE FOR PHASE DIAGRAM MEASUREMENTS

```
5 DEF SEG: POKE &HFE,1
6 REM THIS ROUTINE SAVES DATA FROM BOTH TEMP AND VOLT AND CUTS IT IN HAL
7 REM FIX LINE 580 TO ALTER DATA SAVED
8 REM 315 IS A SLOWING LOOP FOR LONG SETS OF DATA
10 CLS
20 KEY (6) ON :KEY (5) ON
30 KEY 6,"KILL":KEY 5,"PRESET"
35 ON KEY (5) GOSUB 2000
40 KEY 7,"":KEY 8,"":
42 PRINT "HIT F5 FOR PRESET CONDITIONS AND HIT RETURN"
44 PRINT "PLOT UTILITY, TIME OF 1800 SECONDS AND TEMP RANGE OF 20 TO 60"
46 INPUT A$
50 PRINT "DO YOU WANT NUMBERS OR PLOT ? (N OR P)":C$="P"
60 INPUT C$
70 PRINT "WHAT TIME RANGE (1800 secs MAX OF 15000)";
80 INPUT TR
90 PRINT "WHAT TEMPERATURE RANGE"
100 INPUT "LOW END (ZERO)";PL
110 INPUT "HIGH END (100)";PH
120 ON KEY (6) GOSUB 900
130 OPTION BASE 1
140 DIM TM(4000),TP(4000),V(4000)
150 I=0:TO=TIMER
160 CLS
170 DEF SEG=&HD000
180 INIT=0:TRANS=3:REC=6:MYADD%=21:SYSCON%=0
190 CALL INIT (MYADD%,SYSCON%)
195 REM ****TEMPERATURE ROUTINE*****
200 TEMPSET$="REN LISTEN 8 MTA DATA 'C' TALK 8 MLA"
210 CALL TRANS (TEMPSET$,STATUS)
220 IF STATUS%<>0 THEN 950
230 R$=SPACE$(15)
240 CALL REC (R$,LENGTH%,STATUS%)
250 B$=LEFT$(R$,11)
252 GOTO 3000 :REM GET VOLTAGE
255 T1=TIMER-TO
260 IF LENGTH%=15 THEN GOTO 950
270 I=I+1
280 IF T1=>TR THEN 900
300 TM(I)=T1
310 TP(I)=VAL(B$):V(I)=VAL(V$)*200
315 FOR Z=1 TO 5000:NEXT Z
320 IF C$="N" THEN GOSUB 510 ELSE GOSUB 440
330 GOTO 200
340 SOUND 1000!, 18
350 PRINT "DO YOU WANT DATA PRINTED OUT OR ON SCREEN OR NOT AT ALL (P,S,
360 INPUT Q$:IF Q$="N" THEN 400
370 FOR J=1 TO I :IF Q$="P" THEN LPRINT J,"TIME= ";TM(J),"TEMP= ";TP(J)
380 PRINT J,TM(J),TP(J),V(J)
390 NEXT J
400 PRINT "DO YOU WANT TO SAVE DATA TO DISK (Y OR N)"
410 INPUT Q$:IF Q$="N" THEN 620
```

```
410 INPUT Q$:IF Q$="N" THEN 620
420 CLS :GOSUB 530
430 GOTO 620
440 SCREEN 2,0
450 VIEW (0,0)-(639,199)
460 WINDOW (0,PL)-(TR,PH)
470 LINE (0,PL)-(TR,PH),,B
480 PSET(TM(I),TP(I)):PSET(TM(I),V(I))
490 LOCATE 1,5,0,1,1:PRINT I;TM(I);TP(I);V(I);" F6 TO KILL DATA STREAM"
500 RETURN
510 PRINT "TIME= ";TM(I),"TEMP= ";TP(I),V(I),"HIT F6 TO KILL DATA STREAM
520 RETURN
530 PRINT "YOU WILL BE SAVING DATA TO DISK":PRINT:FILES:PRINT
540 PRINT "WHAT IS THE NEW FILE NAME YOU WANT FOR THIS FILE ?"
545 PRINT "REMEMBER, YOU CAN CHANGE TO A OR B DRIVE WITH A\ OR B\ "
550 INPUT F$:F$=F$+".PRN":PRINT:PRINT "YOUR FILE NAME WILL BE ...";F$:PR
560 PRINT "HIT RETURN TO START ":INPUT Q$
570 OPEN F$ FOR OUTPUT AS #2
580 FOR J=1 TO I STEP 1
590 PRINT #2, TM(J),TP(J),V(J)
600 NEXT :CLOSE #2
610 RETURN
620 PRINT:PRINT "DO YOU WISH TO EDIT THE DATA (Y OR N)"
630 INPUT Q$:IF Q$="N" THEN 900
640 DIM D(I)
650 DE=0
660 CLS:PRINT " YOU MAY NOW EDIT THE DATA"
670 FOR J=1 TO I
680 PRINT J,TM(J),TP(J);:INPUT " DELETE (D) ";D$:IF D$="D" THEN D(J)=1
690 NEXT
700 CLS :PRINT "YOU WILL DELETE THE FOLLOWING "
710 FOR J=1 TO I
720 IF D(J)=1 THEN PRINT J,TM(J),TP(J),"D":DE=DE+1
730 NEXT:PRINT "HIT D(ELETE) TO DO SO, ELSE HIT ANY OTHER KEY":INPUT Q$
740 IF Q$<>"D" THEN 620
750 FOR J=I TO 1 STEP -1
760 IF D(J)=1 THEN GOSUB 850
770 NEXT
780 ERASE D
790 CLS:PRINT "THIS IS THE NEW MATRIX OF DATA"
800 I=I-DE
810 FOR J=1 TO I
820 PRINT J,TM(J),TP(J)
830 NEXT
840 GOTO 350
850 FOR K=J TO I
860 TM(K)=TM(K+1):TP(K)=TP(K+1)
870 NEXT
880 RETURN
890 END
900 REM EARLY DATA END - KILL
910 PRINT " ***********DATA ENTRY KILL'ed OR TIME UP ***********"
```

```
910 PRINT " ***********DATA ENTRY KILL'ed OR TIME UP ***********"
920 PRINT "   DO YOU WANT TO WORK WITH THE STORED DATA?   ???? (Y OR N)"
930 INPUT A$:IF A$="Y" THEN GOTO 350
940 END
950 PRINT "ERROR, R$=15 OR STATUS <> 0";STATUS%:SOUND 4000,4
2000 C$="P":PL=20:PH=60:PR=1:TR=1800:GOTO 120
3000 TEMPSET$="REN LISTEN 1 MTA TALK 1 MLA"
3001 REM *****ROUTINE FOR VOLTAGE INPUT******
3100 CALL TRANS (TEMPSET$,STATUS)
3200 IF STATUS%<>0 THEN 950
3300 R$=SPACE$(15)
3400 CALL REC (R$,LENGTH%,STATUS%)
3500 V$=LEFT$(R$,11)
3600 GOTO 255
```

APPENDIX B

SN-G PHASE DIAGRAM DATA

COMPOSITION (w%)	CLOUD POINT (°C)	MONOTECTIC (°C)	CYCLE NO.
0	57.8		
0	58.04		
3.144	57	47	
7.5	46	46	
8.22	49		
8.37	52		
9.02	52.825	47.42	1
9.02	52.436	47.376	2
9.31	53		
14.32	65.884	47.088	1
14.32	62.05	45.904	2
14.32	65.051	44.523	2
14.32	66.864	45.439	1
25.01	97	48	1
25.01	96	48	2
35	83		
93	46	46	

APPENDIX C

STABILITY DIAGRAM DATA

SUMMARY OF PLANAR TO CELLULAR TRANSITIONS

8/4/87 DATE	COMPOSITION	GR.RATE.um/s	THEORETICAL TEMP.GRAD	P/C/D	REAL TEMP.GRAD	G/R
6/30	8.020	0.154	194.718	P	38.944	252.880
CELL 1	8.020	0.276	194.718	P	38.944	141.100
	8.020	0.369	194.718	P	38.944	105.538
	8.020	0.494	194.718	P	38.944	78.833
	8.020	0.884	194.718	P	38.944	44.054
	8.020	1.183	194.718	P	38.944	32.919
	8.020	1.583	194.718	C	38.944	24.601
	8.020	0.884	194.718	P	38.944	44.054
7/2	8.020	0.154	203.440	P	40.688	264.208
CELL 2	8.020	0.884	203.440	P	40.688	46.027
	8.020	1.183	203.440	P	40.688	34.394
	8.020	1.583	203.440	C	40.688	25.703
	8.020	0.884	203.440	P	40.688	46.027
	8.020	1.254	203.440	P	40.688	32.447
	8.020	0.154	117.336	P	23.467	152.384
	8.020	0.494	117.336	P	23.467	47.504
	8.020	0.884	117.336	C	23.467	26.547
	8.020	0.661	117.336	C	23.467	35.503
7/2	8.020	0.154	119.582	P	23.916	155.301
CELL 3	8.020	0.369	119.582	P	23.916	64.814
	8.020	0.494	119.582	P	23.916	48.414
	8.020	0.884	119.582	P	23.916	27.055
	8.020	0.276	119.582	?	23.916	86.653
7/13 C 4	8.020	0.494	182.570	P	36.514	73.915
7/20	16.066	0.276	168.828	P	33.766	122.339
CELL 1	16.066	0.494	168.828	P	33.766	68.351
	16.066	0.884	168.828	C	33.766	38.196
	16.066	0.884	171.757	C	34.351	38.859
	16.066	0.276	171.757	C	34.351	124.462
7/23	16.066	0.154	175.371	?	35.074	227.754
CELL 2	16.066	0.494	175.371	C	35.074	71.000
7/31	12.202	0.276	165.725	P	33.145	120.091
CELL 1	12.202	0.884	165.725	C	33.145	37.494
	12.202	0.494	165.725	P	33.145	67.095
	12.202	0.994	165.725	C	33.145	33.345
	12.202	0.701	165.725	C	33.145	47.282
	12.202	0.494	165.725	C	33.145	67 095
8/3 C 2	12.202	0.494	174.360	P	34.872	70 591
8/3	12.202	0.661	180.836	P	36.167	54.716
CELL 3	12.202	0.884	180.836	C	36.167	40.913
	12.202	2.835	180.836	BC	36.167	12.757
	12.202	1.583	180.836	BC	36.167	22.847

APPENDIX D

COMPUTER PROGRAM FOR MEASUREMENT OF INTERCELLULAR SPACINGS

```
10 CLS
20 PRINT "GRAPHIC TABLET OUTPUT, HIT f10 TO STOP PROGRAM"
30 KEY (10) ON
40 ON KEY (10) GOSUB 300
50 KEY 10,"STOP"
60 PRINT "you will measure cell size in inches"
70 M=1:I=0
80 INPUT "INPUT PHOTO MAGNIFICATION _________",M
85 INPUT "INPUT SPECIMEN ID_________________",ID$
90 OPTION BASE 1
100 DIM X(25),Y(25),D(200)
110 OPEN "COM1:9600,N,8,2,CS,DS" AS 1
120 LINE INPUT #1,A$
130 B$=MID$(A$,2,1)
140 IF LEN(A$)=13 THEN B$=LEFT$(A$,1)
150 I=I+1
160 X(1)=VAL(MID$(A$,3,6))/1000
170 Y(1)=VAL(MID$(A$,9,6))/1000
180 PRINT X(1),Y(1)
190 LINE INPUT #1,A$
200 B$=MID$(A$,2,1)
210 IF LEN(A$)=13 THEN B$=LEFT$(A$,1)
220 X(2)=VAL(MID$(A$,3,6))/1000
230 Y(2)=VAL(MID$(A$,9,6))/1000
240 D(I)=(SQR((X(1)-X(2))^2+(Y(1)-Y(2))^2))/M
250 REM goto 300 if time to stop
260 GOSUB 380
270 SOUND Y(1)*1000+.5,2
280 GOTO 120
290 SOUND 1000!, 18
300 CLS
301 PRINT "DO YOU WANT DATA PRINTED OUT OR ON SCREEN OR NOT AT ALL (P,S,
310 INPUT Q$:IF Q$="N" THEN 340
320 FOR J=1 TO I:IF Q$="P" THEN LPRINT " D= ";D(J)," ID= ";ID$
325 PRINT J,D(J)
330 NEXT J
340 PRINT "DO YOU WANT TO SAVE DATA TO DISK (Y OR N)"
350 INPUT Q$:IF Q$="N" THEN 550
360 CLS :GOSUB 460
370 GOTO 550
380 CLS
381 SCREEN 2,0
390 VIEW (0,0)-(639,199)
400 WINDOW (0,0)-(10995/1000,10995/1000)
410 PSET(X(1),Y(1))
411 PSET(X(2),Y(2))
420 LOCATE 1,5,0,1,1:PRINT X(1);Y(1),X(2);Y(2),D(I)
430 RETURN
440 PRINT "D=";D(I)
450 RETURN
460 PRINT "YOU WILL BE SAVING DATA TO DISK":PRINT:FILES:PRINT
470 PRINT "WHAT IS THE NEW FILE NAME YOU WANT FOR THIS FILE ?"
```

```
470 PRINT "WHAT IS THE NEW FILE NAME YOU WANT FOR THIS FILE ?"
480 INPUT F$:F$=F$+".PRN":PRINT:PRINT "YOUR FILE NAME WILL BE ...";F$:PR
490 PRINT "HIT RETURN TO START ":INPUT Q$
500 OPEN F$ FOR OUTPUT AS #2
505 PRINT #2,$ID
510 FOR J=1 TO I
520 PRINT #2, D(J)
530 NEXT :CLOSE #2
540 RETURN
550 END
```

APPROVAL

CELLULAR SOLIDIFICATION IN A MONOTECTIC SYSTEM – CENTER DIRECTOR'S DISCRETIONARY FUND FINAL REPORT

By W. F. Kaukler and P. A. Curreri

The information in this report has been reviewed for technical content. Review of any information concerning Department of Defense or nuclear energy activities or programs has been made by the MSFC Security Classification Officer. This report, in its entirety, has been determined to be unclassified.

E. A. TANDBERG-HANSSEN
Director, Space Science Laboratory